

- Fret 5914



This is to certify that the

thesis entitled

Corrugated Board As A Package Cushioning Material

presented by

Eric Christian Wenger

has been accepted towards fulfillment of the requirements for

Master degree in Packaging

Major professor

Date 2-17-94

O-7639

MSU is an Affirmative Action/Equal Opportunity Institution



PLACE IN RETURN BOX to remove this checkout from your record. TO AVOID FINES return on or before date due.

DATE DUE	DATE DUE	DATE DUE
44 0 9 1 /98		
4265m		
2 2080		
9/20 8 A 30 2502		

MSU is An Affirmative Action/Equal Opportunity Institution cyclesdatedus.pm3-p.1

CORRUGATED BOARD AS A PACKAGE CUSHIONING MATERIAL

By

Eric Christian Wenger

A THESIS

Submitted to

Michigan State University

in partial fulfillment of the requirements

for the degree of

MASTER OF SCIENCE

School of Packaging

1994

ABSTRACT

CORRUGATED BOARD AS A PACKAGE CUSHIONING MATERIAL

By

Eric Christian Wenger

The performance of corrugated fiberboard as a cushioning material was investigated and a mathematical approach to predict the peak acceleration, number of useful drops, dynamic deflection, and shock duration was tested and confirmed. Cushions in the flat and edge crush mode were conditioned at different moisture contents and subjected to drop tests in order to obtain shock transmission data over the intended range of use. The method was an energy approach based on the development of dynamic stress vs. strain curves for the material. Because of strain rate effects, an approach which related drop parameters to dynamic stress and strain data was essential. This resulted in a high degree of correlation between predicted and actual results. Conventional cushion curves for corrugated were generated from a single stress vs. strain curve following recommended ASTM procedures. Corrugated cushions were also compared to existing foam cushions both in performance and economics, and were found to be very competitive.

ACKNOWLEDGEMENTS

I would like to thank Dr. Gary Burgess as my advisor for his knowledgeable insights, timely advice, and keen sense of humor.

I would also like to thank Dr. Paul S. Singh and Dr. Bob Ofoli for their time and support as committee members.

I would also like to thank those at the School of Packaging who took time to offer their help and friendship during the course of this challenging and rewarding endeavor.

TABLE OF CONTENTS

LIST OF TAB	LES	V
LIST OF FIGU	JRES	vi
LIST OF SYM	BOLS	Х
CHAPTER 1	••••••	1
INTROL	DUCTION AND LITERATURE REVIEW	1
1.1 1.2	Introduction	1 2
CHAPTER 2	••••••	14
	ETICAL DEVELOPMENT, MATERIALS,	14
2.1	Theoretical Predictions Predicting the Number of Useful Drops	14 25
	Prediction of Impact Durations	31
	Performance Under High Humidity Conditions	32
	Cushion Curves for Corrugated Board	35
2.1.5	Materials and Storage Conditions	36
2.3	Drop Test	36
2.4	Flat and Edge Crush Tests	40
CHAPTER 3	•••••••••••••••••••••••••••••••••••••••	42
RESULT	S	42

3.1	Edge Crush Data	42
3.2	Flat Crush Data	52
CHAPTER 4		65
DISCU	SSION AND CONCLUSIONS	65
4.1	Utility of Method	65
4.2	Experimental Errors	66
4.3	Analysis of Results	69
4.4	Comparing With Other Cushioning Materials	70
4.5	Future Work	72
APPENDICE	S	
APPEN	DIX A	73
APPEN	DIX B	76
APPEN	DIX C	79
APPEN	DIX D	81
REFERENCE	S	83

LIST OF TABLES

ГАВ	TABLE F	
1.	Humidity factors for corrugated board	33
2.	Dynamic stress and strain versus energy absorption data for C-flute in the edge crush mode @ 50% RH	43
3.	Energy absorption versus dynamic stress data for C-flute in the edge crush mode at various humidity conditions	49
4.	Energy absorption versus dynamic strain data for C-flute in the edge crush mode at various humidity conditions	50
5.	Validation test for cushions in the edge crush mode	53
6.	Dynamic stress and strain versus energy absorption data for C-flute in the flat crush mode @ 50% RH	56
7.	Energy absorption versus dynamic stress data for C-flute in the flat crush mode at various humidity conditions	60
8.	Energy absorption versus dynamic strain data for C-flute in the flat crush mode at various humidity conditions	61
9.	Validation test for cushions in the flat crush mode	62
10.	Comparing the performance of corrugated board to other cushioning materials	71

LIST OF FIGURES

FIGURE		PAGE
1.	Cushion curve data for Arcel 310	3
2.	Crossection of a Honeycomb cushion	4
3.	A typical stress vs. strain curve for Honeycomb	6
4.	Corrugated cushion in the flat crush mode	10
5.	Corrugated cushion in the edge crush mode	11
6.	Comparison of static and dynamic force vs. compression curve	15
7.	Static compression test of block cushion. The force F is uniformly distributed over area A	17
8.	Force vs. compression curve for block cushion	17
9.	Energy absorption characteristics of a cushion	19
10.	Dynamic stress vs. strain curve for cushion	21
11.	Change in dynamic strain between two points on the dynamic stress vs. strain curve	23
12.	Falling weight striking block held between two walls	27

13.	Energy absorption of a cushion subjected to multiple impacts	29
14.	Energy absorption for a cushion subjected to multiple impacts	30
15.	Diagram of test equipment used for drop tests	38
16.	Typical shock waveform	39
17.	Dynamic stress vs. energy for C-flute in the edge crush mode @ 50% RH	45
18.	Dynamic strain vs. energy for C-flute in the edge crush mode @ 50% RH	47
19.	Dynamic stress vs. strain for C-flute in the edge crush mode @ 50% RH	48
20.	Cushion curve for 12" drop for C-flute board in edge crush mode @ 50% RH	54
21.	Dynamic stress vs. energy for C-flute in flat crush mode @ 50% RH	57
22.	Dynamic strain vs. energy for C-flute in flat crush mode @ 50% RH	58
23.	Dynamic stress vs. strain for C-flute in flat crush mode @ 50% RH	59
24.	Cushion curve for 12" drop for C-flute board in flat crush mode @ 50% RH	64
25.	Unfiltered shock waveform	67
26.	Filtered shock waveform	68
27.	Shock pulse from edge cushion subjected to 1st	73

28.	Shock pulse from edge cushion subjected to 2nd	74
29.	Shock pulse from edge cushion subjected to last drop conditions	75
30.	Shock pulse from flat cushion subjected to 1st	76
31.	Shock pulse from flat cushion subjected to 2nd	77
32.	Shock pulse from flat cushion subjected to last	78
33.	Cushion curve for 24" drop for C-flute board in edge crush mode @ 50% RH	79
34.	Cushion curve for 36" drop for C-flute board in edge crush mode @ 50% RH	80
35.	Cushion curve for 18" drop for C-flute board in flat crush mode @ 50% RH	81
36.	Cushion curve for 24" drop for C-flute board in flat	82

LIST OF SYMBOLS

force, (lb) F W weight, (lb) G acceleration expressed as a multiple of gravity acceleration due to gravity, (386.4 in/sec) g $\mathbf{d}_{\mathbf{m}}$ dynamic compression, (in) stress, (psi) σ strain, (inches/inch) ε load bearing area, (inch²) Α d static compression, (in) thickness, (in) t volume, (inch³) V drop height, (in) h static loading, (psi) S dynamic stress, (psi) σ_{m} dynamic strain, (inches/inch) ε_m

buckling stress, (psi) $\sigma_{ ext{min}}$ average stress, (psi) σ_{avs} change in strain, (inches/inch) $\Delta \varepsilon$ change in energy absorbed, (psi) ΔA mass of object, (lbm) m V_{i} impact velocity, (in/sec) V_{r} rebound velocity, (in/sec) coefficient of restitution e maximum energy absorbing capacity, (psi) max N number of useful drops impact duration, (msec) t_{dur} time from beginning of impact to peak G, (msec) t_{o-pk} time from peak G to end of impact, (msec) t_{pk-o} dynamic stress at 50% RH σ_{ref} dynamic strain at 50% RH ε_{ref} impact duration at 50% RH tref gate time, (msec) GT

C

constant

CHAPTER 1

INTRODUCTION AND LITERATURE REVIEW

1.1 INTRODUCTION

The purpose of this study is to develop a method for predicting the cushioning performance of corrugated fiberboard. Although it is one of the most widely used packaging materials for containment, it has generally been ignored as a performance oriented cushioning material. Its traditional use has been in the production of shipping containers, or as dunnage in the packaging of rugged items where product fragility is of little concern [1]. The ease of recyclability and separation from other materials makes corrugated board an ideal alternative to the highly visible foam materials which have been scrutinized by environmental legislation in recent years. However, no research aimed at quantifying the cushioning ability of the material has been published to date. Some research has been done on Honeycomb cushioning, which is a paper based cushioning material used mainly by the military. Cushion curves for Honeycomb at standard laboratory conditions were developed by Singh [2] in 1986. Asvanit [3] furthered the study of Honeycomb in 1988 by assessing the effects of moisture content on shock transmission properties.

Several models have been developed for predicting the behavior of polymeric cushions. Burgess [4] formulated a model for closed cell cushions based on the thermodynamic processes associated when partially trapped air is compressed rapidly in an elastic network of interconnected membranes. Throne and Progelhof [5] have also researched the static and dynamic stress vs. strain behavior of low density closed cell cushions.

The development of a model for corrugated cushions allows an engineer to reduce dozens of cushion curves, which take into account product weight, expected drop height, cushion thickness, and bearing area, to a few descriptive equations which can be solved through mathematical manipulation or by the use of sophisticated curve fitting software. A typical set of cushion curves for Arcel 310 is shown in Figure 1. A single cushioning material may require a dozen or more of these curves to reasonably describe its behavior over the intended range of use. It is these advantages which provide the incentive for this work.

1.2 LITERATURE REVIEW

From 1953 to 1959, the Structural Mechanical Research Laboratories at the University of Texas, under contract with the Delivery Quartermaster Research and Development command [6], had investigated several types of cushioning materials to be used for single drop aerial deliveries. Honeycomb was chosen as the material best suited for this purpose. Its structure consists of a core of oval cells bounded on both sides by linerboard face panels. Figure 2 illustrates a crossectional view of its structure.

Figure 1: Cushion curve data for Arcel 310 [18].

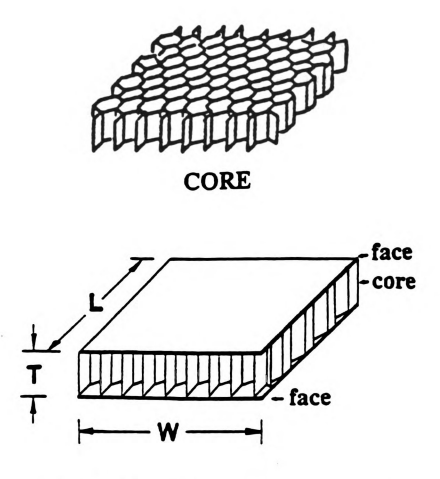


Figure 2: Crossection of a Honeycomb cushion [3].

Honeycomb is made entirely from unbleached Kraft linerboard paper. The core is made from 33 pound basis weight stock, while the face panels consist of 69 pound linerboards. Dynamic stress vs. strain curves were investigated to provide information on the energy absorption characteristics, and from this, the cushioning properties of the material were assessed. In 1986, cushion curves were experimentally developed by Singh [2] under standard lab conditions of 72°F @ 50% RH. This research was aimed at evaluating the effects of cell size, cushion thickness, and drop heights on transmitted shocks. In 1988, Asvanit [3] furthered the research by developing cushion curves for Honeycomb exposed to various moisture contents. It is from this body of knowledge that many behavioral characteristics of the material were derived. Both the material and the method of analysis are similar to corrugated material.

The most important analysis tool is the static stress vs. strain curve. A typical static stress vs. strain curve for Honeycomb is shown in Figure 3. Examination of the curve reveals three distinct modes of behavior the material undergoes during static compression. During initial loading, the stress increases linearly until a sharp peak is reached. The Honeycomb is compressed elastically throughout this region, showing no visible signs of deformation. As the core starts to buckle, the stress values decrease and maintain a nearly constant value until a strain of around 65% is reached. At this level of strain, the cells have completely collapsed and the cushion acts like a solid block of paper under compaction. This region, where the cushion has effectively "bottomed out", is marked by a sharp rise in stress values as the applied load is increased.

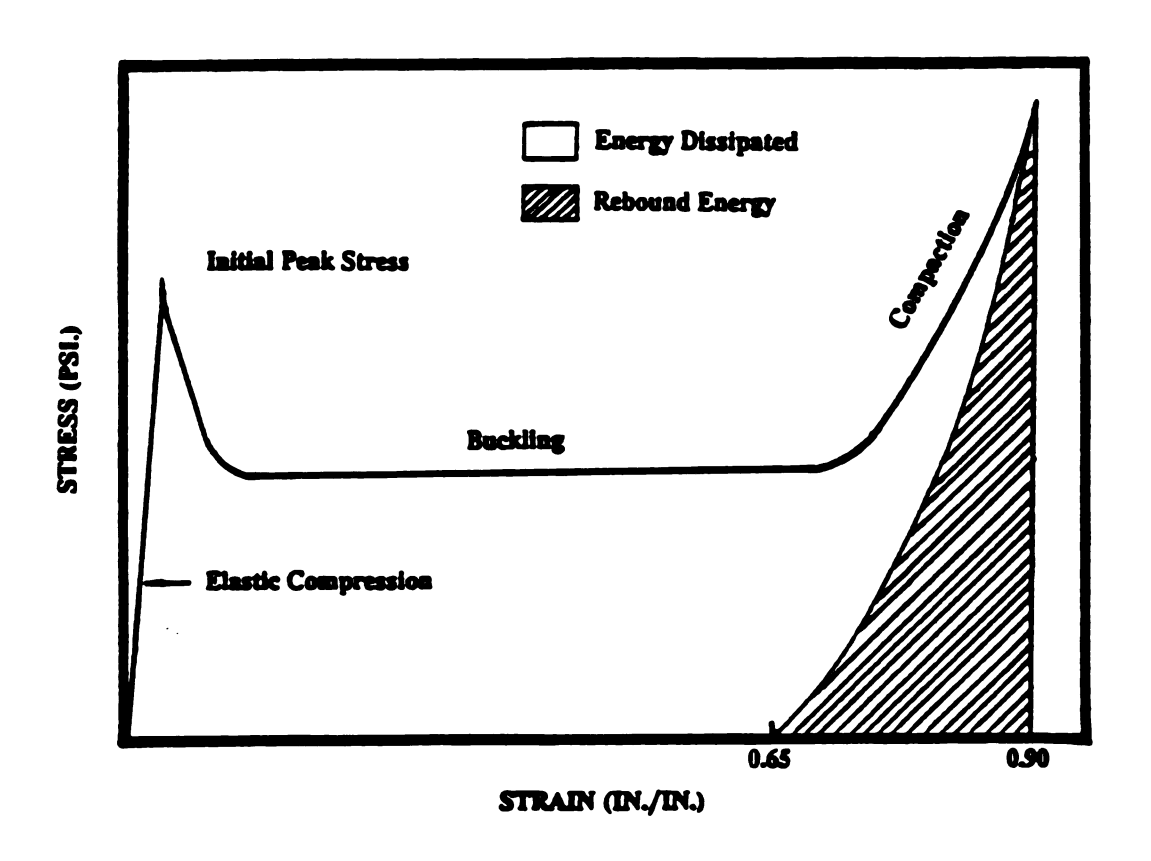


Figure 3: A typical stress vs. strain curve for Honeycomb [3].

The energy absorbed by a cushion during compression is the area under the stress vs. strain curve up to the point of compression. This will be shown in detail later on. When compressed, a cushion either stores or dissipates energy. In Honeycomb, the amount of stored elastic energy is small compared to the total energy absorbed during impact since the elastic range is very small. The stress vs. strain curve during unloading is shown in Figure 3 as the cross-hatched area, which equals the elastic energy recovered by a cushion during the rebound stage of an impact. The ratio of rebound to dissipated energy is called the resilience [6], which is considered a material property related to shock absorption ability. A material with high resilience will not necessarily provide optimum protection for an item, simply because the large amount of rebound energy present in the cushion subjects the object to repeated impacts. Honeycomb cushioning is considered an excellent material for single drop use because it has low resilience and is a good dissipater of impact energy. The same is expected to be true of corrugated. The smallest decelerations can be obtained within the constant stress region of the static stress vs. strain curve. Witting [7] recommends a minimum of 0.2 inch pre-compression on Honeycomb material to overcome the initial peak stress, however if complete crushing of the cushion is expected, the pre-compression is not necessary.

The dynamic stress vs. strain curves obtained from five grades of Honeycomb material produced results similar in shape to the static curves, except the dynamic stresses were somewhat higher [8]. The difference between the static and dynamic stress for a given strain depends on cell size, cushion density, and processing techniques. Honeycomb grades are measured by overall density related to cell size, basis weights used, and

percent resin impregnation. Karnes tested five untreated grades and found that for core densities ranging from 1.0-2.6 lb/ft³, the dynamic energy absorption averaged around 44% higher than its static counterpart. The maximum strain under dynamic test conditions at the point of bottoming out was about 2-5 percent higher than the static maximum strain value.

There have been numerous studies on the factors which affect the compression strength of corrugated fiberboard. From these investigations, the edge and flat crush tests were developed as a means of measuring the compressive resistance of the material. The edge crush test, ASTM D 2808-90 [9], measures the edgewise compressive strength of a short column of combined corrugated fiberboard. Research has linked the compressive resistance of specimens along with the flexural stiffness of the board to the top-to-bottom compression strength of corrugated containers [10]. The flat crush test, TAPPI T808 om-86 [11], measures the resistance of flutes to a crushing force applied perpendicular to the surface of the board. Flat crush is a measure of flute rigidity within the board. Both tests are often used for comparing different lots of similar combined boards, or for comparing different basis weights combinations.

A pilot study [12] was conducted which aimed at relating the cushioning properties of C-flute corrugated board to the flat and edge crush values of the material. A summary of the methods used for the experiment follows. Newton's second law states that:

$$F = W \times G \tag{1}$$

where: F =force W =weight

G = acceleration expressed as a multiple of gravity, g g = acceleration due to gravity = 386.4 in/sec²

Applying this to a dynamic drop with a product weight W, and solving for G yields:

$$G = \frac{F}{W} \tag{2}$$

Newton's third law states that when a body exerts a force on another body, the latter exerts a force of equal magnitude and opposite direction on the former. Thus, the falling weight produces a downward force F on the corrugated board, and the board exerts a force equal in magnitude but directed upward on the weight as the reaction force. Figures 4 and 5 illustrate typical flat and edge cushions used for the pilot study. In an edge cushion, the opposing force is limited to the edge crush strength of the material and can be quantified by:

$$F = edge crush (lb/in) \times edge length (in)$$
(3)

The "edge length" for a cushion is the total length of board the falling weight acts upon. For example, a ten layer cushion where each layer has a length of 2.5" would have an "edge length" of 25". Equation (2) then becomes:

Edge crush
$$G = \frac{\text{edge crush}(\text{lb/in}) \times \text{edge length}(\text{in})}{\text{product weight}(\text{lb})}$$
 (4)

The same method is used to derive the flat crush equation. The reaction force is given by:

$$F = \text{flat crush (psi)} \times \text{bearing area (in}^2)$$
 (5)

Substitution into equation (2) yields:

Flat crush
$$G = \frac{\text{flat crush}(\text{psi}) \times \text{bearing area}(\text{in}^2)}{\text{product weight}(\text{lb})}$$
 (6)

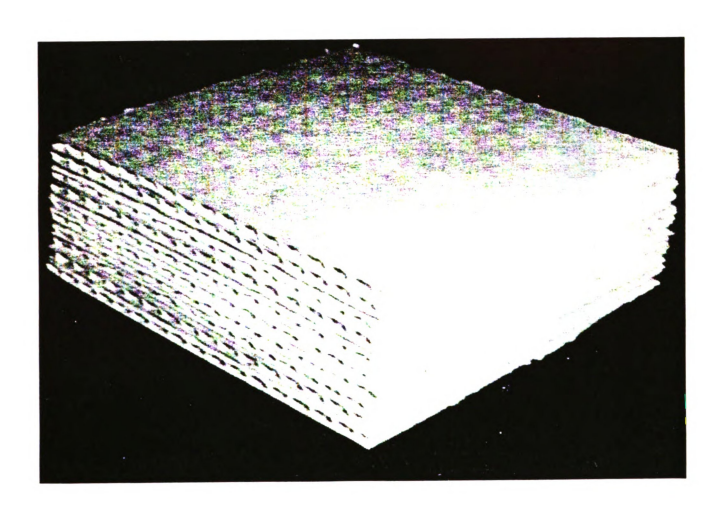


Figure 4: Corrugated cushion in the flat crush mode.

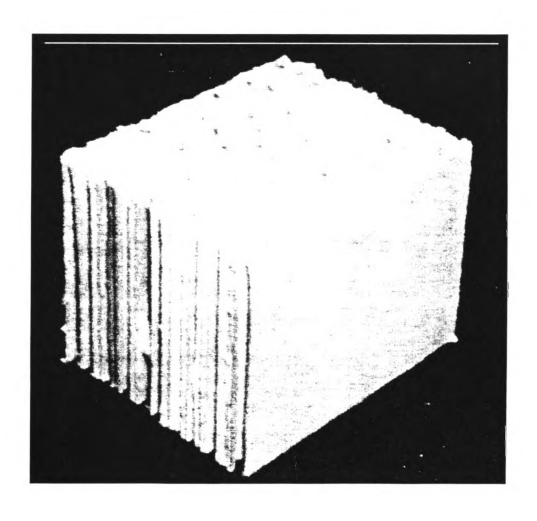


Figure 5: Corrugated cushion in the edge crush mode.

An obvious concern regarding equation (6) is how the number of layers in a flat cushion affects the peak G in a drop. According to equation (6), peak G is independent of the number of layers used provided the cushion does not bottom out. If it bottoms out however, the predictions are invalid, and this is determined by examining the dynamic compression in a drop. In order to calculate dynamic compression, the following energy balance is manipulated:

Potential energy = weight \times drop height = force \times dynamic compression Solving for dynamic compression gives:

$$d_m = \frac{\text{product weight (lb)} \times \text{drop height (in)}}{\text{force (lb)}}$$
 (7)

where: $d_m = \text{dynamic compression}$

Substituting the forces from equations (3) and (5) gives:

$$d_m = \frac{\text{product weight (lb)} \times \text{drop height (in)}}{\text{edge crush (lb/in)} \times \text{edge length (in)}}$$
(8)

$$d_m = \frac{\text{product weight (lb)} \times \text{drop height (in)}}{\text{flat crush (psi)} \times \text{bearing area (in}^2)}$$
(9)

for edge crush and flat crush cushions respectively.

If it is assumed that the force required to crush corrugated remains relatively constant throughout the dynamic compression, then drops made onto corrugated cushions should result in relatively constant accelerations. Hence, an acceleration vs. time waveform should be a square wave, resembling a waveform produced by a shock machine when dropped onto its gas programmers.

Flat and edge crush tests were performed according to the standards cited earlier, and average values were calculated for both. It was verified that the number of layers had no affect on the flat crush strength. The above predictions were tested on manually constructed corrugated cushions and it was found the equations did not accurately predict peak G's resulting from dynamic drops. Predictions were found to be in error up to \pm 50% of actual results. This large error was unexpected however, as this method did work well for Honeycomb material. This can be attributed to the incorrect assumption that a constant force is required to crush a specimen throughout the entire dynamic compression. Hence, constant accelerations will not result, and the predictions are invalid. Thus, another approach must be taken in order to accurately predict peak G's associated with drops made onto corrugated cushions.

CHAPTER 2

THEORETICAL DEVELOPMENT, MATERIALS, AND TEST METHODS

2.1 THEORETICAL PREDICTIONS

This chapter outlines a method which allows all the cushion curves for a material to be generated using the dynamic force vs. compression curve. We would like to be able to use static force vs. compression data, but the "sluggish" response of most materials to deformation prevents this information from being useful. Viscoelastic materials have stresses which are dependent upon the strain rate as well as the strain. Figure 6 shows a comparison between static and dynamic force vs. compression curves for a typical material. The two curves are usually similar in shape, but can have very different values. The dynamic curve for a material is always higher than its static counterpart. If a material is non-viscoelastic and light weight (i.e. low density), then the two curves can be expected to be almost identical. However, for materials which are viscoelastic or high density in nature, the curves may show large differences. Hence, the static curve cannot be used to predict peak G's with any success. Although corrugated material is nonviscoelastic and lightweight, the dynamic curve should be used if possible. However, obtaining such a curve by conventional means is nearly impossible, as it would require a compression tester capable of operating at impact speeds of around 100 in/sec, instead of the standard 1/2" per minute.

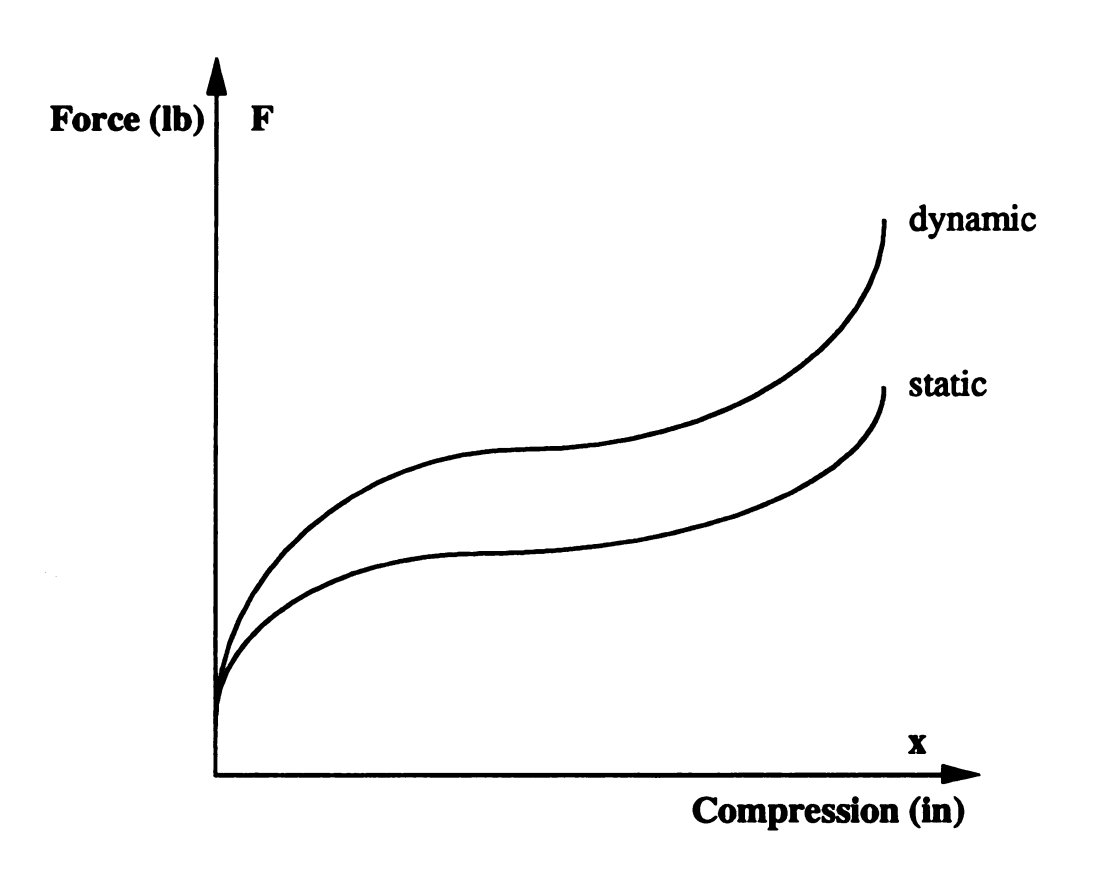


Figure 6: Comparison of static and dynamic force vs. compression curve.

Instead, the dynamic curve will be deduced from actual drop tests. The generation of the static force vs. compression curve will serve as the starting point, and it is here an explanation of the technique will begin.

A compression test is first performed on a block of material of arbitrary dimensions and thickness. This is shown in Figure 7. The static force F acting on the cushion is assumed to be evenly distributed over the entire bearing area A. From this, force vs. compression can be plotted for the test cushion. A typical force vs. compression curve is illustrated in Figure 8. This curve can be converted to a static stress vs. strain curve by the following equations:

$$stress \ \sigma = \frac{force}{area} \tag{10}$$

$$strain \ \varepsilon = \frac{compression}{thickness} \tag{11}$$

The stress vs. strain curve has the same general shape as the force vs. compression curve, because the conversion merely involves the operation of scaling both axes to the proper units. The stress vs. strain curve is a material property, which applies to cushions of any size, whereas the original force vs. compression curve applies only to the specific cushion tested, provided the material is homogeneous (i.e. same composition throughout). Corrugated board does not first appear to be homogeneous, as it contains both a medium and linerboards. However, in the flat crush orientation the liners are not compressible, so they play no role in the results. In the edge crush orientation, both the medium and liners are compressed, but the composition remains uniform throughout the entire thickness because all crossections are identical. Thus, corrugated board can be considered

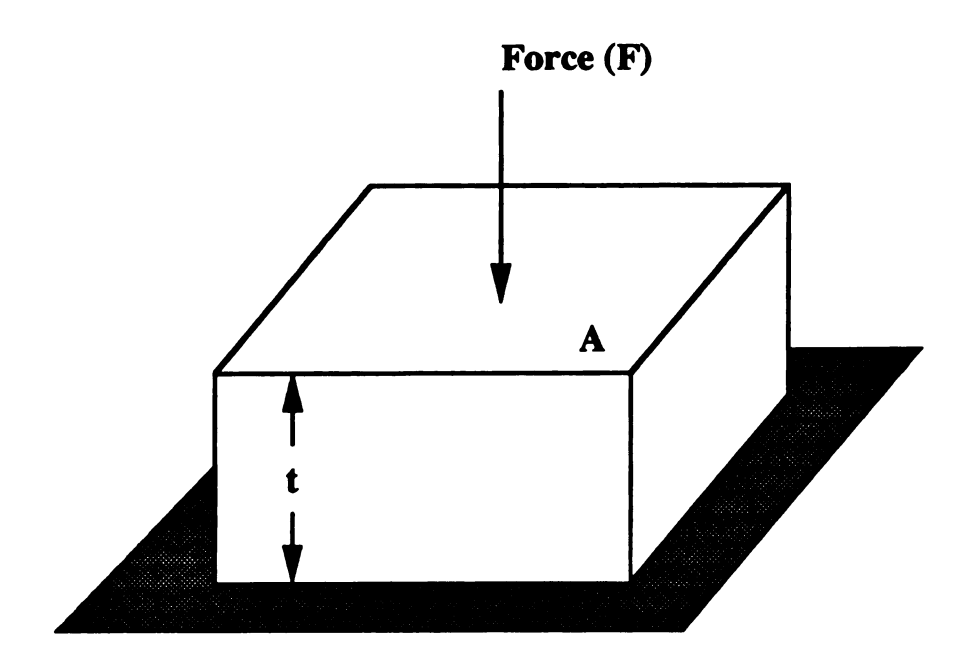


Figure 7: Static compression test of block cushion. The force F is uniformly distributed over area A.

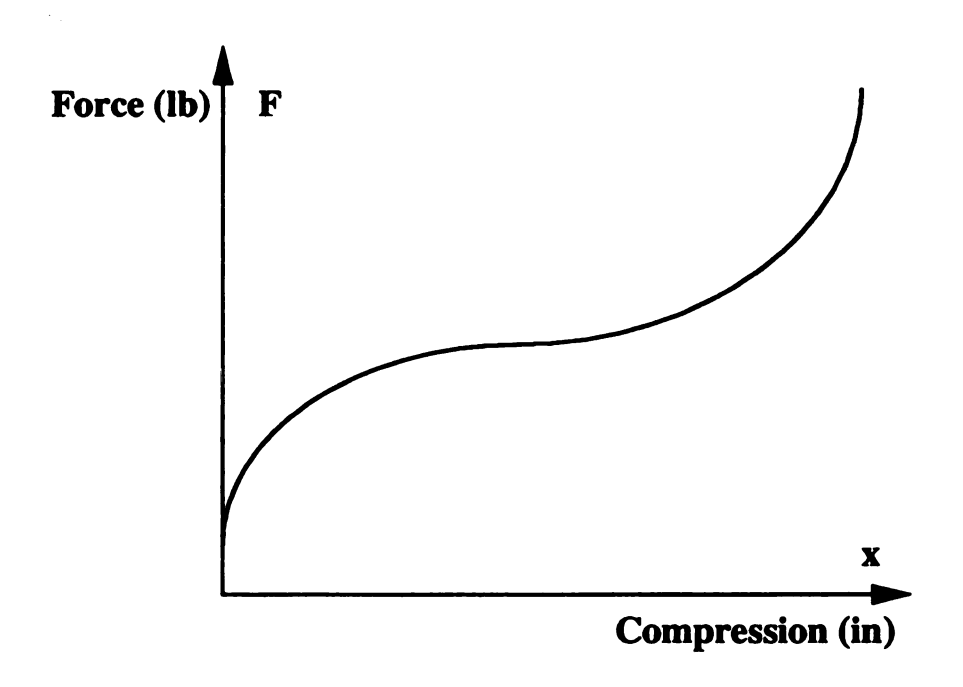


Figure 8: Force vs. compression curve for block cushion.

homogeneous, and the stress vs. strain curve can be applied to cushions of variable size and thickness.

The energy absorbed by a cushion during compression is the area under the force vs. compression curve up to a particular deflection. Inspection of Figure 9 shows the force is continuously changing with respect to compression. The energy absorbed by a cushion can then be expressed by:

Energy absorbed =
$$\int_{0}^{d} F dx$$
 (12)

where: F =force d =compression

But according to equations (10) and (11),

$$force = stress \times area \tag{13}$$

$$compression = strain \times thickness$$
 (14)

which leads to,

Energy absorbed =
$$\int_{0}^{\varepsilon} (\sigma A)(t d\varepsilon) = At \int_{0}^{\varepsilon} \sigma d\varepsilon = V \int_{0}^{\varepsilon} \sigma d\varepsilon$$
 (15)

where: $\sigma = \text{stress}$

 $\varepsilon = \text{strain}$

A = Area

t =thickness

V = Volume

Simply stated, the area under the force vs. compression curve is equal to the area under the stress vs. strain curve multiplied by the cushion volume.

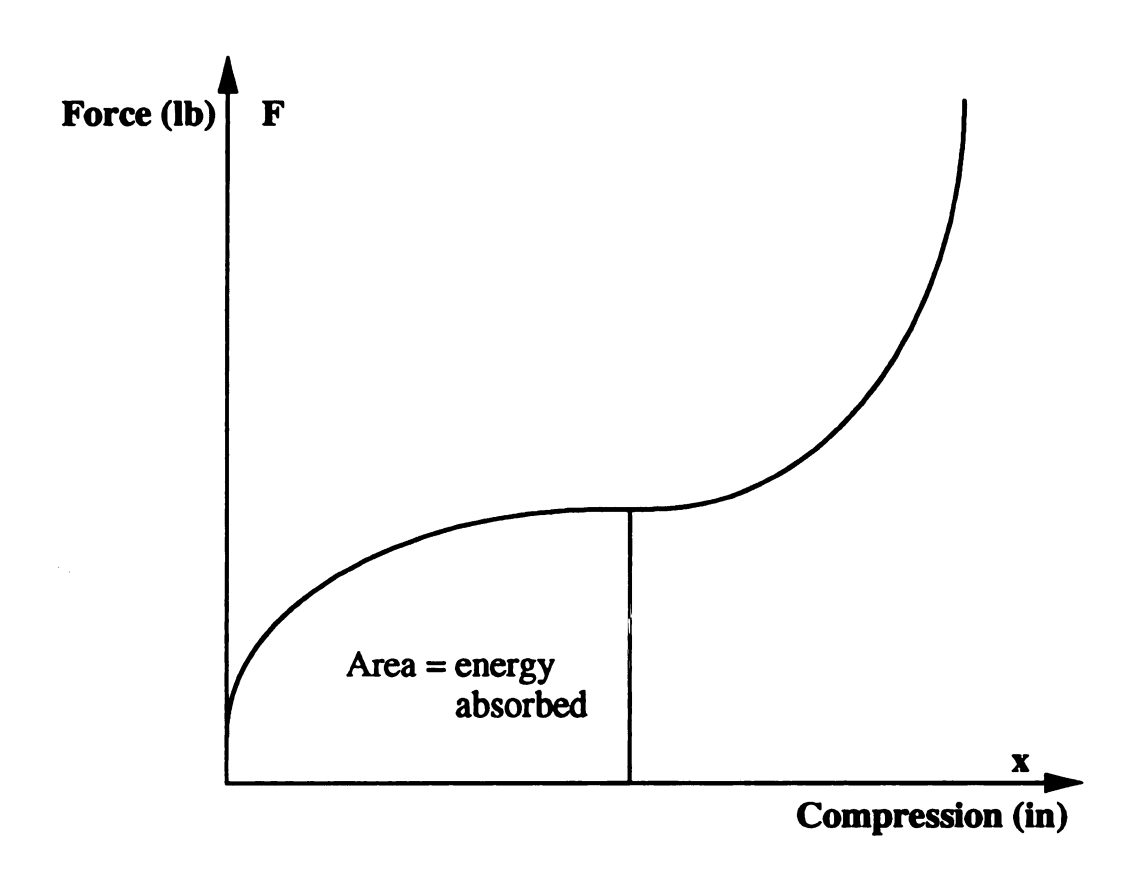


Figure 9: Energy absorption characteristics of a cushion.

The above discussion used the static force vs. compression curve to develop the result in equation (15). The discussion also applies to the dynamic force vs. compression curve, with stress accounting for the strain rate affects. Hence, even though the dynamic curve cannot be obtained by conventional means, the results can still be applied to a drop situation. In order to relate absorbed energy to drop parameters, the following is manipulated:

Potential energy = weight \times drop height = energy absorbed by cushion

 $W \times h = At \times$ Area under dynamic stress vs. strain curve

Solving for the area under the curve yields:

Area under stress vs. strain curve
$$=\frac{W \times h}{A \times t} = \frac{s \times h}{t}$$
 (16)
where: $s = \frac{W}{A} = \text{static loading (psi)}$

Once the dynamic stress vs. strain curve for a material is obtained either by experimental or theoretical methods, it is possible to locate where an impact lies on the curve by moving along the strain axis until an area equal to sh/t is enclosed, as shown in Figure 10. Once the energy absorbed in an impact is known, the peak acceleration can be found from the corresponding dynamic stress σ_m . Equation (2) can be changed over to stress parameters using equation (13), yielding:

$$G = \frac{F}{W} = \frac{\sigma_m \times A}{W} = \frac{\sigma_m}{s} \tag{17}$$

Thus, in dynamic impacts with known parameters (i.e. drop height, static loading, and cushion thickness), dynamic stress values can be found. The drop parameter sh/t is simply the energy per cubic inch of material to be absorbed by the cushion. This determines the dynamic stress for the stress vs. strain curve, and peak G is calculated using equation (17). The only

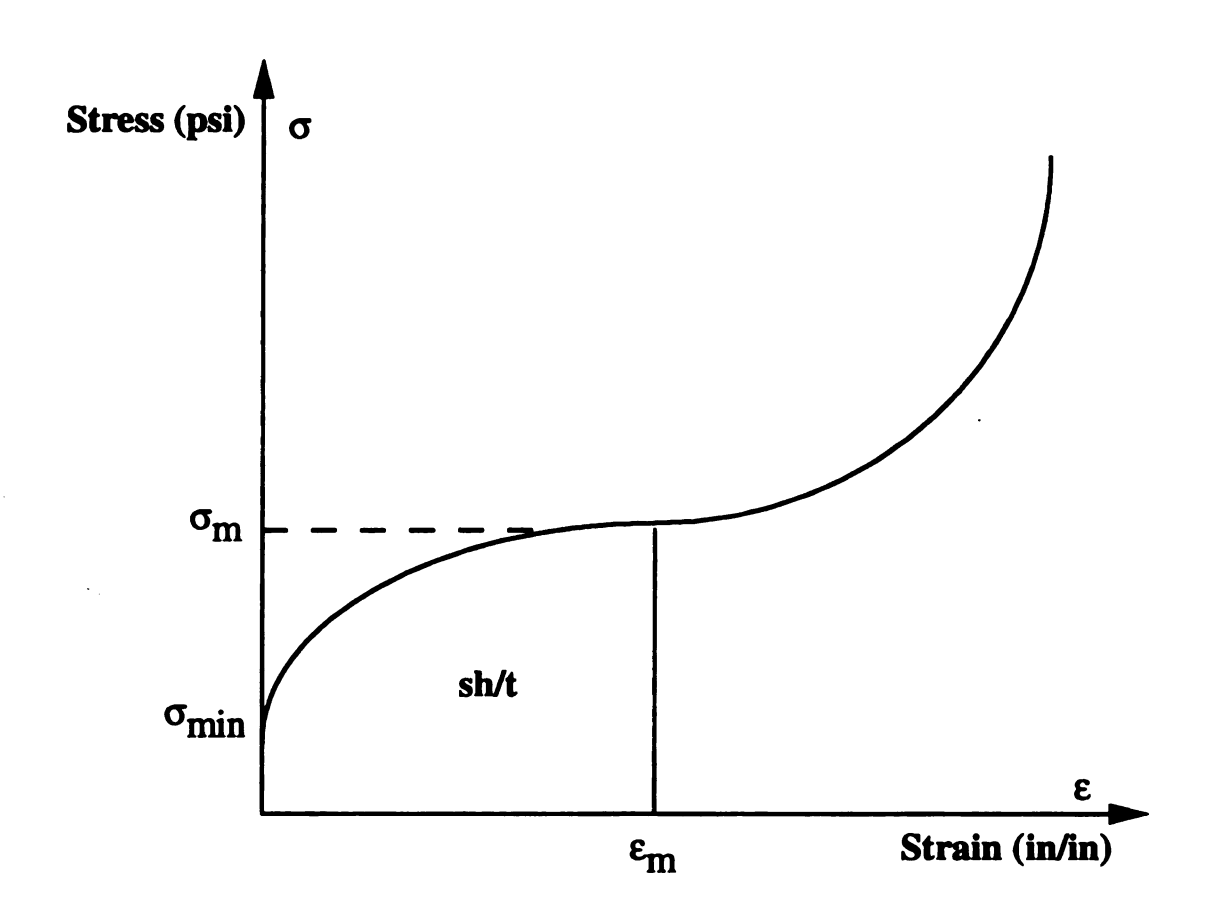


Figure 10: Dynamic stress vs. strain curve for cushion.

trouble at this point is that the dynamic stress vs. strain curve is not known and in general cannot be obtained from the static stress vs. strain curve.

Fortunately, the dynamic stress vs. strain curve can be experimentally developed through drop tests. To start, block cushions are constructed. The first specimen is subjected to drop conditions which result in a small amount of absorbed energy (sh/t). The drop is made and the peak deceleration is recorded. Equation (17) is then used to derive the first dynamic stress value corresponding to the area sh/t. Subsequent tests are performed on cushions which are forced to absorb increasing amounts of energy. This is continued, and the sh/t (area) values are tabulated against Gs (dynamic stress) values in ascending order. The stress values do not approach zero when the absorbed energy is zero because a minimum stress level must be overcome in order for a cushion to be compressed. Once this stress is exceeded, the structure buckles and begins to compress.

Once the dynamic stress vs. area values have been found, the strain values may be calculated. Figure 11 shows the change in energy absorption as the cross-hatched area between successive test points on the curve. The change in area can be approximated by the trapezoid rule:

$$\Delta A = \Delta \varepsilon \times \sigma_{avg} = \Delta \varepsilon \times \left[\frac{\sigma_1 + \sigma_2}{2} \right]$$
 (18)

Solving for $\Delta \varepsilon$ yields:

$$\Delta \varepsilon = \left[\frac{\Delta A}{\frac{\sigma_1 + \sigma_2}{2}} \right] \tag{19}$$

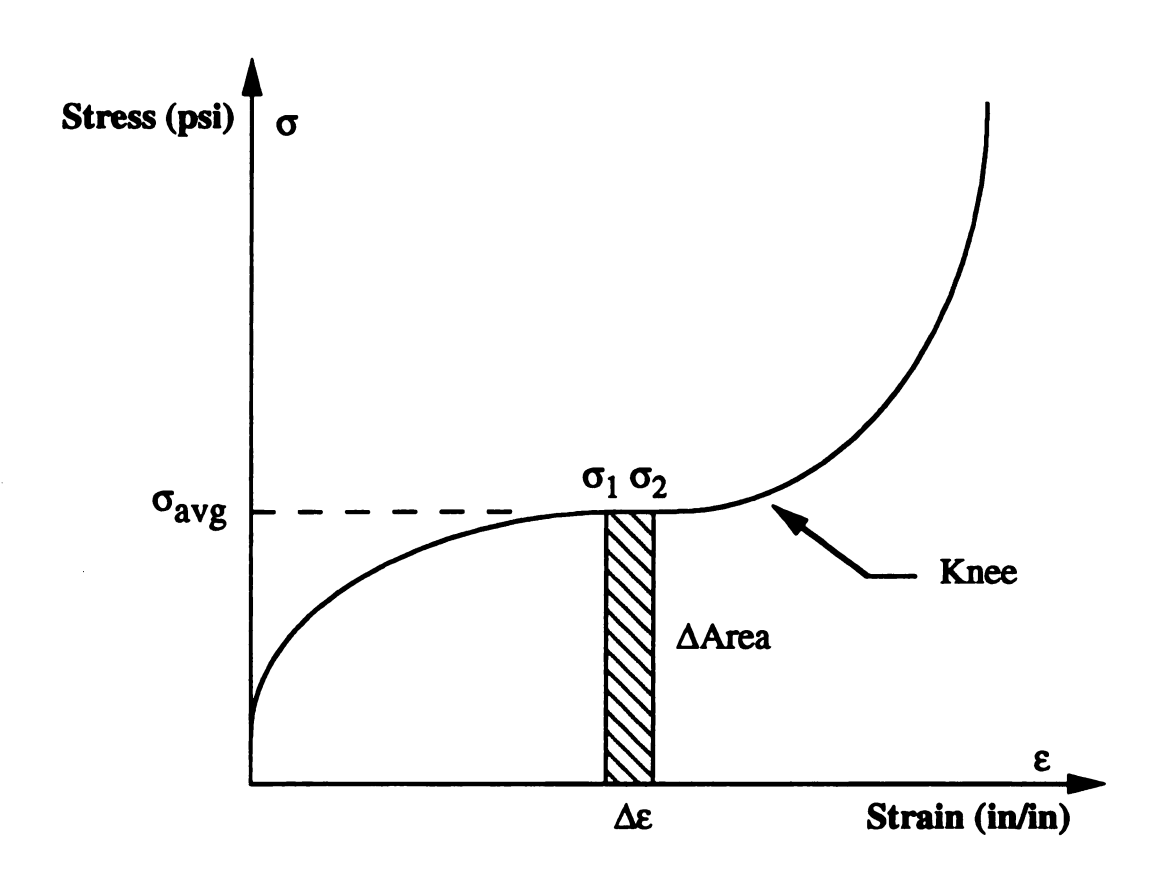


Figure 11: Change in dynamic strain between two points on the dynamic stress vs. strain curve.

where: $\Delta \varepsilon$ = change in dynamic strain

 σ_1 = dynamic stress at 1st test point

 σ_2 = dynamic stress at 2nd test point

 σ_{avg} = average stress between two points = $(\sigma_1 + \sigma_2)/2$

 ΔA = change in energy absorbed

Equation (19) allows the change in strain between any two neighboring points on the dynamic stress vs. strain curve to be found. From this, the next strain can be calculated using:

$$\varepsilon_2 = \varepsilon_1 + \Delta \varepsilon \tag{20}$$

where: ε_1 = dynamic strain corresponding to σ_1 ε_2 = dynamic strain corresponding to σ_2

Once a starting value for strain is known, equation (20) can be used to find every other strain. The strains can then be calculated for every dynamic stress value. The experimental data is then plotted, thereby revealing the general shape of the curve. At this point, there are three quantities which are related: stress, strain, and area. By using special curve fitting software, polynomial equations representing the plotted data can be generated. The more useful approach is to plot both dynamic stress and strain as a function of energy absorbed. In this way dynamic stress, strain, and peak acceleration may be predicted based on the energy absorbed by the test cushion.

The polynomial equations can be used to calculate all relevant information related to particular drop events. First, values are chosen for static loading, drop height, and cushion thickness. The sh/t value is then plugged into the polynomial which relates dynamic stress to energy absorbed by the cushion. Solving this equation gives dynamic stress, and peak G is found by using equation (17). This same sh/t value is then plugged into the polynomial

relating dynamic strain to energy absorbed. Applying the resulting strain to equation (14) can then be used to find the dynamic compression resulting from the drop.

2.1.2 PREDICTING THE NUMBER OF USEFUL DROPS

Corrugated cushions can only be subjected to a limited number of impacts before losing their cushioning ability, as they experience permanent deformation after only a single drop. It is important, therefore, to be able to predict the number of drops a cushion can withstand before bottoming out, along with the peak G's associated with these multiple impacts. Before either of these can be predicted, it is necessary to discuss some fundamental properties of materials which exhibit permanent set upon exposure to dynamic forces. The coefficient of restitution "e", defined as the ratio of rebound velocity to impact velocity, is used as a measure of the energy lost in an impact. To quantify the energy lost, the following energy balance is used:

Potential energy of falling object = Kinetic energy just before impact

$$w \times h = \frac{1}{2} m v_i^2 \tag{21}$$

where: m = mass of object

 $v_i = \text{impact velocity (in/sec)}$

w =weight of object = mg

Kinetic energy just after rebound =
$$\frac{1}{2}mv_r^2$$
 (22)

where: v_r = rebound velocity (in/sec)

But $v_r = e \times v_i$ so,

Kinetic (rebound energy) =
$$\frac{1}{2}m(ev_i)^2 = \frac{1}{2}me^2v_i^2 = e^2wh$$
 (23)

Energy lost = impact - rebound =
$$wh - e^2wh = wh(1 - e^2)$$
 (24)

The fraction of energy lost in an impact can then be expressed by:

Fraction of energy lost =
$$\frac{\text{final energy}}{\text{initial energy}} = \frac{wh(1-e^2)}{wh} = (1-e^2)$$
 (25)

Equation (25) is the key result used to handle multiple impacts. Figure 12 shows a model which will be used to explain how the above results are applied to inelastic materials which incur permanent deformation upon exposure to dynamic forces. When the falling weight strikes the block, it must first bottom out the spring before it can be displaced. Compressing the spring corresponds to recoverable elastic energy and moving the block represents unrecoverable energy (permanent deformation). If the drop energy wh is insufficient to bottom out the spring, then the block does not move and there is no permanent deformation. This corresponds to a perfectly elastic drop (e = 1). If sufficient drop energy exists, then the block moves and there is some permanent deformation. In the worst case, all of the impact energy is lost in the drop. This corresponds to a perfectly plastic drop (e = 0). When $0 \le e \le 1$, the falling weight strikes the block with impact energy wh, and rebounds with energy e^2 wh. This is true for all subsequent identical drops made onto the block.

This same analogy can be used to describe the behavior of corrugated cushions. In a dynamic drop, a cushion absorbs energy wh, but gives back energy e²wh during rebound. This will be true for every drop made onto a given cushion, until it absorbs enough energy to cause it to bottom out. The amount of absorbed energy which causes a cushion to "barely" bottom out,

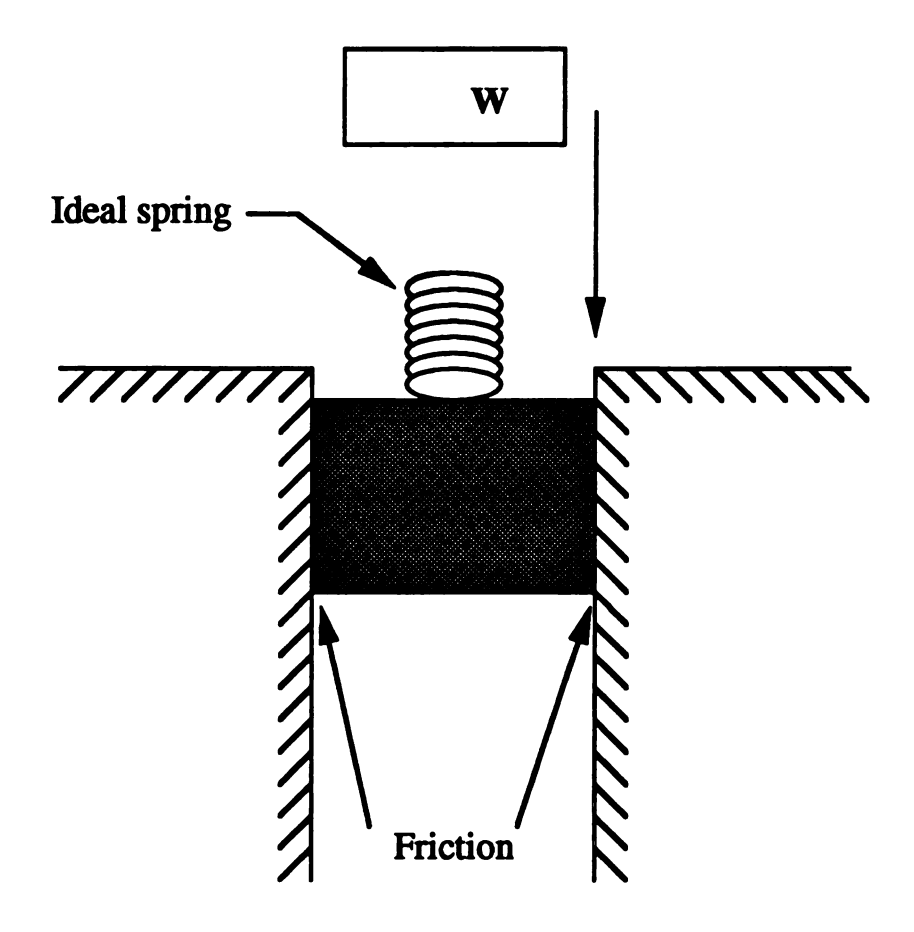


Figure 12: Falling weight striking block held between two walls by friction.

either as the result of a single drop or combination of drops can be obtained from the dynamic stress vs. strain curve. This quantity can be visually represented as the area under the stress vs. strain curve up to the point where the stress values start to rapidly increase, shown as the "knee" on the curve in Figure 11.

The energy absorbed (i.e. area under stress vs. strain curve) for a typical corrugated cushion subjected to multiple impacts under identical drop conditions is shown in Figure 13. As outlined earlier, the cushion absorbs energy in the amount wh in the first drop, but gives back e^2 wh. Hence, this same quantity of energy must be reabsorbed in the second impact to get back to point 1 on the stress vs. strain curve. During the second drop, the cushion then absorbs wh $(1-e^2)$, according to equation (24). Solving for area under the curve yields:

$$A_2 = \frac{wh(1-e^2)}{At} = \frac{sh(1-e^2)}{t}$$
 (26)

In other words, an additional quantity of energy in the amount of $(1-e^2)$ sh/t must be absorbed with each new impact. This is illustrated in Figure 14.

The peak deceleration for the first impact is found simply by dividing the dynamic stress σ_1 by the static loading. To find the dynamic stress for the second impact, the additional energy absorbed $(1-e^2)$ sh/t must be added to the sh/t from the first, thereby moving further out along the strain axis with each additional impact. Peak G for the second drop is found by dividing the new dynamic stress σ_2 by the static loading. This is continued

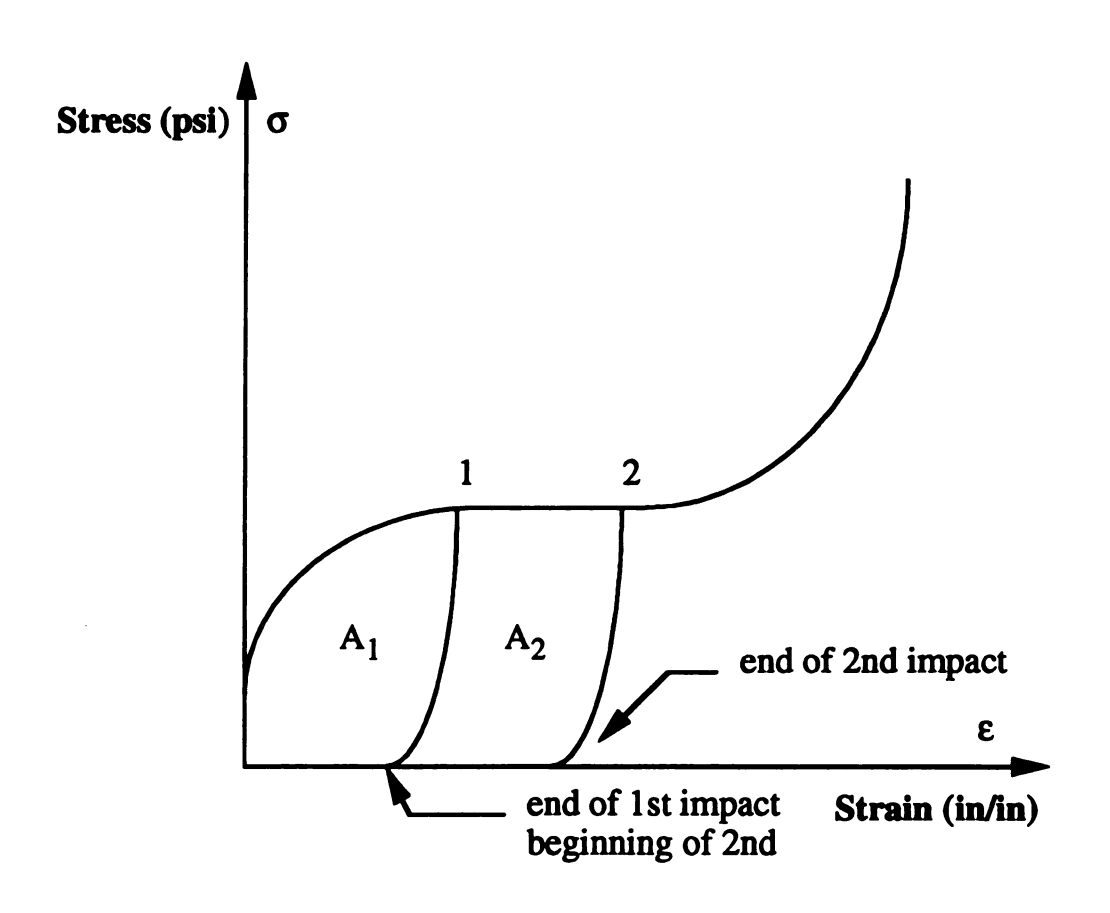


Figure 13: Energy absorption of a cushion subjected to multiple impacts.

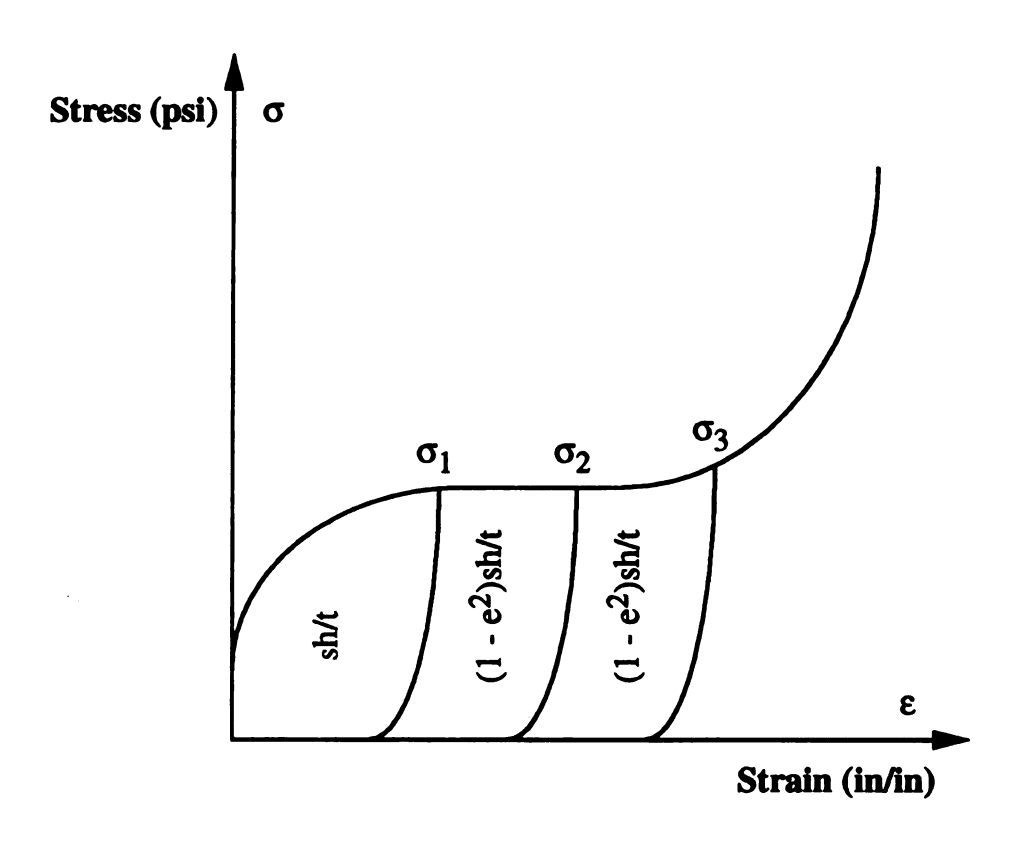


Figure 14: Energy absorption for a cushion subjected to multiple impacts.

until the cushion absorbs enough energy to exceed the maximum. As the cushion "bottoms out", the peak G rises dramatically and the useful life of the cushion is exhausted. The number of useful drops N for a cushion under identical drop conditions can be determined by setting the total amount of energy to be absorbed, $\sinh(t+(N-1)(1-e^2)\sinh/t$, equal to the maximum energy absorbing ability of the cushion and solving for N, which gives:

$$N = 1 + \frac{1}{(1 - e^2)} \left[\frac{\max}{sh/t} - 1 \right]$$
 (27)

where: sh/t = energy absorbed in an arbitrary impact max = maximum energy absorbing ability of cushion (psi)

2.1.3 PREDICTION OF IMPACT DURATIONS

The impact duration can be estimated for any drop made onto a corrugated cushion once the dynamic stress vs. strain relationship is known. However, because the stress continuously changes as the cushion compresses, the calculation is complicated. The impact duration will be split into two parts; the deceleration phase in which the mass slows to a stop from its impact velocity, and the acceleration phase in which the mass goes from rest to its rebound velocity. In order to simplify the analysis, it will be assumed that the object undergoes constant acceleration during both parts of the impact. Under constant acceleration, an objects velocity increases linearly with time. Hence, the following is true:

displacement = average velocity × time

$$d_m = \left(\frac{V_i + 0}{2}\right) \times t_{o-pk} \tag{28}$$

Solving for t_{o-pk} yields,

$$t_{o-pk} = \frac{2d_m}{V_i} \tag{29}$$

where: d_m = dynamic compression (in) V_i impact velocity = $\sqrt{2gh}$

The linear spring mass model will be used to find the time from peak G to the end of the impact. Under this model, the time duration for the deceleration and acceleration phases are equal. The total impact duration can then be estimated by:

$$t_{dur} = t_{o-pk} + t_{pk-o} = 2\left(\frac{2d_m}{V_i}\right) = \frac{4d_m}{V_i}$$
 (30)

2.1.4 PERFORMANCE UNDER HIGH HUMIDITY CONDITIONS

Packages are exposed to a wide spectrum of environmental conditions when shipped through the distribution system. Hence, it is important to know how these environments affect the performance of corrugated cushions. Previous work by Hoph [13] on Honeycomb cushions showed that exposure to high humidities lowered the stress values on the static stress vs. strain curve; consequently the energy absorption characteristics of the material were diminished as well. Table 1 shows the effect of various humidities on box compression strength [10]. The humidity factor H is used to adjust the

Table 1: Humidity factors for corrugated board [10].

Relative Humidity	H
Dry	125%
25%	110%
50%	100%
75%	80%
85%	60%
90%	50%

compression strength of a box, depending on the relative humidity of the environment the container is exposed to. As relative humidity increases, the compression strength is reduced from the value at standard conditions (50% RH). Conversely, the compression strength of a container will increase when the relative humidity is less than standard conditions. Thus, 50% RH is used as a reference value (H = 1). Because these factors were developed for box compression strength, which involves crushing the material, these same humidity factors can be applied to the experimentally determined dynamic stresses. The stress value at any relative humidity can be calculated by:

$$\sigma = \sigma_{ref} \times H \tag{31}$$

where: σ = dynamic stress at arbitrary relative humidity σ_{ref} = dynamic stress at 50% RH H = humidity factor

Similarly, strain values can be found at any relative humidity by:

$$\varepsilon = \frac{\varepsilon_{ref}}{H} \tag{32}$$

where: ε = dynamic strain at arbitrary relative humidity ε_{ref} = dynamic strain at 50% RH

For example, if the cushions are exposed to a relative humidity of 75%, then all the stress values on the curve will decrease by 20%, while the strains are increased by 20%. It follows then that lower peak accelerations are obtained for identical drops made at higher humidity conditions. While this is good, the drawback is that cushions will "bottom out" in fewer drops than those exposed to lower humidity conditions. The impact durations are also affected by exposure to higher humidities, as the dynamic compression values will be greater for identical drops made at higher humidities. Under

identical drop conditions, impact durations at higher humidities are related to those at standard conditions by:

$$t_{dur} = \frac{t_{ref}}{H} \tag{33}$$

where: t_{dur} = impact duration at arbitrary relative humidity t_{ref} = impact duration at 50% RH

2.1.5 CUSHION CURVES FOR CORRUGATED BOARD

Conventional cushion curves for first impacts of corrugated cushions can be generated from dynamic stress vs. energy absorbed data. The first step is to select a drop height for which the cushion curve is to be developed. Next, construct vertical (peak G's) and horizontal (static loading) axes, and divide each into suitable increments. Once a cushion thickness is chosen, calculate the energy absorbed (sh/t) for each of the static loading increments. Then obtain the dynamic stress values for each sh/t, and divide by the corresponding static loading to get peak G for each drop. A plot can then be constructed with peak G's on the vertical axis, and static loading on the horizontal axis. A "best fit" curve should then be drawn through each point to obtain the cushion curve for that particular thickness. This procedure can then be repeated for other drop heights and cushion thicknesses, thereby revealing the performance of the material over the intended range of use. This will be done for C-flute corrugated board both in the flat and edge crush orientations.

2.2 MATERIALS AND STORAGE CONDITIONS

Materials: In this study, flat and edgewise cushions were constructed so as to test the material's cushioning performance both parallel and perpendicular to the direction of flutes. C-flute corrugated board was used to make the cushions for this experiment. The individual layers of each specimen were held together by 3M Brand Sprayment Adhesive, which was used to minimize warpage of the samples. Cushions were conditioned in two different temperature and humidity environments and allowed to reach equilibrium with the ambient atmosphere. The two environments were:

- a) 72 ± 1°F @ 50% RH (Standard Conditioning Atmosphere)
- b) 100 ± 1 °F @ 80% RH

which resulted in different moisture contents within the samples.

Apparatus: Humidity chambers were used to condition the samples at the higher temperature and humidity conditions. The chambers remained closed for the entire conditioning period, so as to minimize humidity fluctuations to that inherent of the equipment $(\pm 3\%)$.

Method: All cushions were conditioned in accordance with ASTM D4332-89 [14], which recommends a minimum exposure time of seventy two hours for the samples to reach equilibrium. The cushions were cut using a S & S corrugated sample cutter and a Milwaukee Model LN 62A610 band saw. These were used to provide the cushions with a loading surface parallel to the free moving platen of the cushion tester.

2.3 DROP TEST

Materials: Several cushion sizes were constructed for the drop test, depending on the desired static loading. Drop heights, ballast weights, and

cushion dimensions were however, constrained within the practical limits of the cushion tester.

Apparatus: The equipment used for the drop test consisted of the following:

- 1. A Lansmont Corporation Model 23 cushion tester with a flat dropping head onto which ballast weights could be added, a lifting mechanism, and a rebound brake trigger switch. Figure 15 illustrates the equipment used.
- 2. A Dytran piezoelectric accelerometer containing a sensitivity of 10 mV/g was mounted onto the free moving platen.
- 3. A Dytran Model 4110 AC piezotron charge amplifier was used to magnify the accelerometer output.
- 4. A Lansmont Corporation Testpartner Version 2 data acquisition software system was used to record shock pulse waveforms from the accelerometer mounted on the cushion tester's moving platform as it impacted the corrugated cushions. The waveforms were filtered at a frequency of 50 Hz in order to remove the high frequency components associated with the ringing of the test fixture that were superimposed on the underlying shock pulses. A trigger level of \pm 20 g's was used to prevent small accelerations not originating from the actual impact from being recorded on the acceleration time history. Figure 16 illustrates a typical shock waveform.
- 5. Lansmont Corporation lubricant was applied to minimize frictional forces between the guide rods and the falling platen during drop testing. However, because these forces cannot be eliminated completely, equivalent drop heights based on the impact velocity were used in place of actual drop heights. The cushion tester contains an adjustable gate which measures the time, in milliseconds, for a blade width equal to one half an inch to pass

38

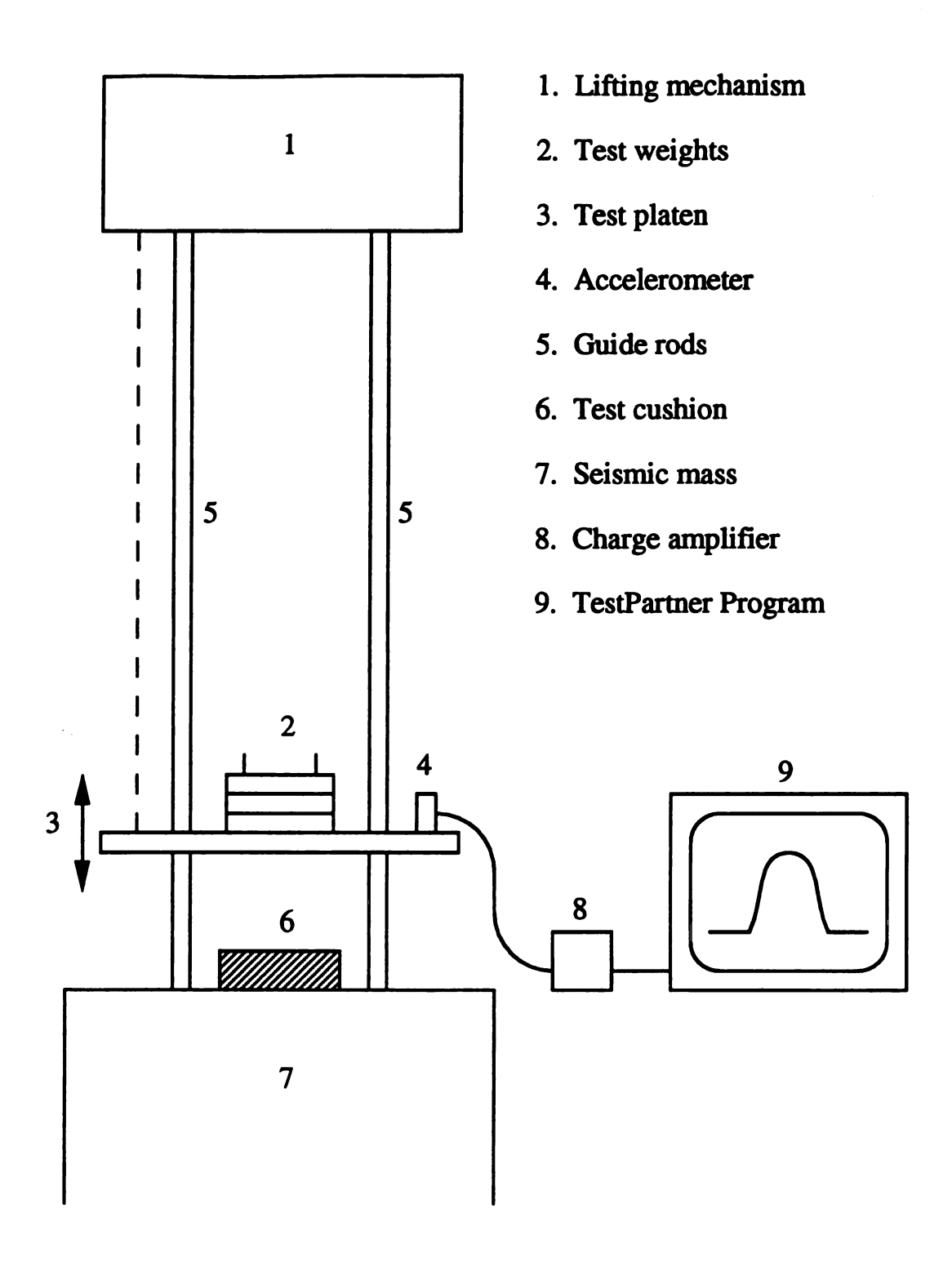


Figure 15: Diagram of test equipment used for drop tests.

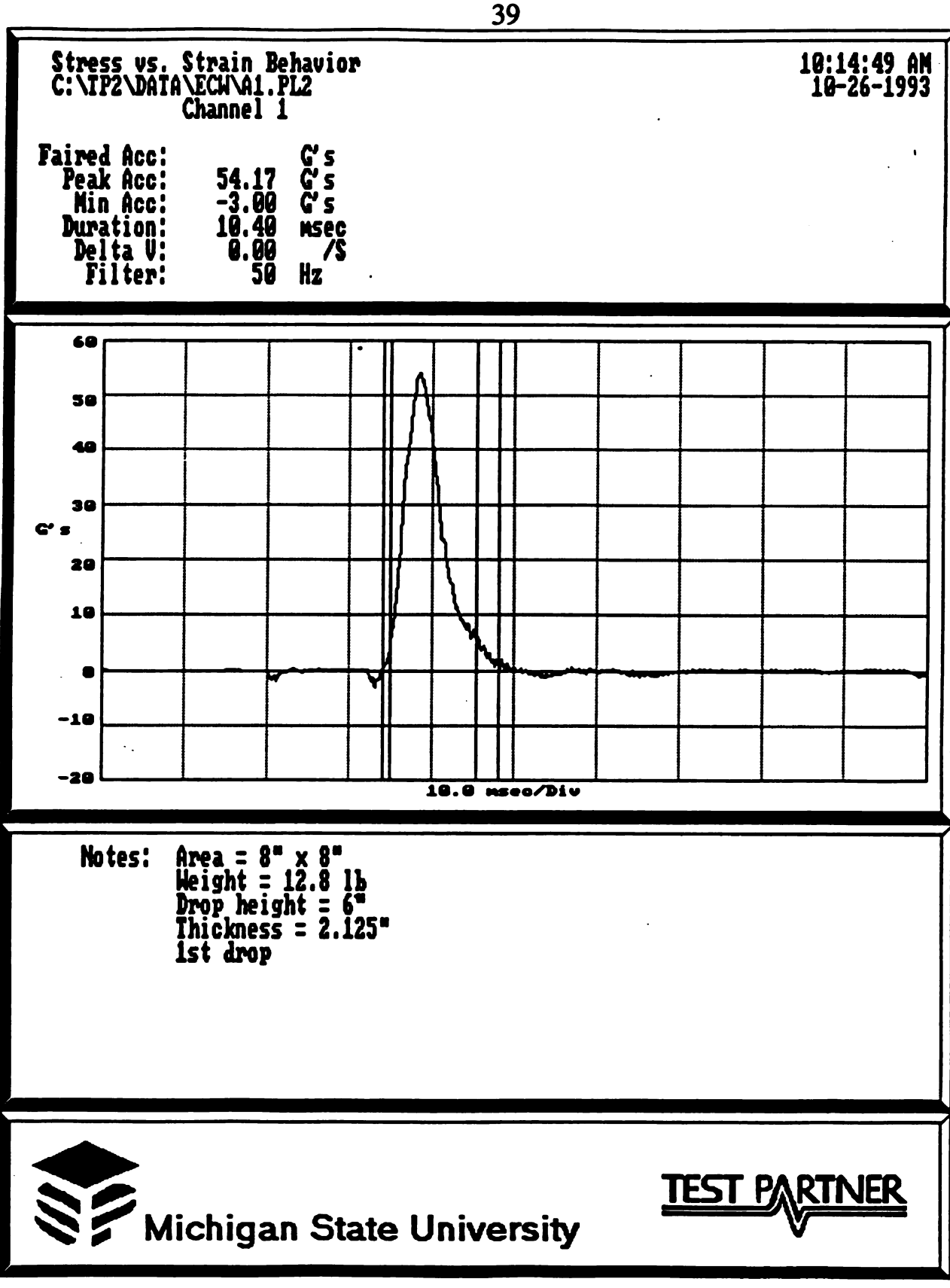


Figure 16: Typical shock waveform.

through it. This time interval, known as the "Gate Time", can be expressed by:

$$GT = \frac{blade\ width}{V_i} = \frac{0.5"}{\sqrt{2gh}}$$
 (34)

Thus, to make a drop from an arbitrary height, an equivalent drop height must be used which satisfies equation (34).

Method: ASTM D1596-91 [15], the method for determining the dynamic shock cushioning characteristics of packaging materials, was followed in this experiment. However, since corrugated fiberboard cushions experience permanent deformation after only a single drop, replicate samples were used for each drop made on the cushion tester. A total of five drops per static loading were made in order to increase the statistical accuracy of the results.

2.4 FLAT AND EDGE CRUSH TESTS

Materials: Flat and edge crush tests were performed on C-flute corrugated fiberboard samples according to TAPPI Standard T808 om-86 and ASTM D2808-90 respectively.

Apparatus: The equipment used to perform these tests consisted of:

- 1. A 400 Series TMI Crush Tester, Model no. 17-36.
- 2. A TMI standard circular sample cutter.
- 3. A TMI standard edge crush sample cutter.

Methods: Twenty specimens each were cut and stored at standard conditioning atmosphere ($72 \pm 1^{\circ}F$ @ 50% RH) for a minimum of 72 hours to allow the samples to reach the equilibrium moisture content of the ambient atmosphere. Tests were then conducted in accordance with the

applicable standards, with the exception that the loading edges of the edge crush samples were not dipped in molten paraffin as specified in the standard. It was deemed that by not following this procedure, the samples would be subjected to forces which were closer in nature to those experienced during the drop tests.

CHAPTER 3

RESULTS

3.1 EDGE CRUSH DATA

Table 2 summarizes the various drop conditions that were used to develop the energy absorbed vs. dynamic stress and strain relationships for edge crush cushions conditioned at 50% RH. The data is arranged in ascending order so that the relationships may be shown graphically and analyzed using special curve fitting software. Appendix A contains a portion of the original shock pulses used to generate the table. Fortunately, only a few are needed to illustrate the procedure used to generate the data. It is important to note that the stress, strain, and energy absorbed data can be applied to any drop situation because they represent a property of the material (i.e. like density), whereas the rest of the data relates to the particular drop conditions used for each test.

For example, the drop parameters for the first test cushion are: h = 2", w = 12.8 lb, A = 19.5 in², and t = 1.5". Using equation (17), the dynamic stress is $47.864 \times (12.8/19.5) = 31.42$ psi. This process was repeated in order to calculate the remaining stress values. Once all of the stresses have been found, the strain values are calculated using equations (19) and (20). Recall equation (19) gives the change in dynamic strain between two test points on

Table 2: Dynamic stress and strain versus energy absorption data for C-flute in the edge crush mode @ 50%RH.

		Cushion		Peak G		Energy Absorbed	Stress	Strain
Weight (lb) Area (sq. in.)	Area (sq. i	n.)	Thickness (in)	in drop	e	s*h/t (psi)	G*s (psi)	(in/in)
12.8 4.875 x 4	4.875	۲4	1.5	47.864	0.53	0.875	31.42	0.0279
12.8 1.625 x 4	1.625 x	4	1.5	42.344	0.49	2.626	83.39	0.0584
17.8 1.625 x 4	1.625 x	4	1.5	43.052	0.42	5.477	117.9	0.0867
27.8 1.625 x 4	1.625 x 4	_	1.5	34.81	0.33	11.405	148.88	0.1311
27.8 1.625 x 3	1.625 x 3		1.5	28.208	0.28	15.207	160.86	0.1557
38.4 1.625 x 3	1.625 x 3	_	1	21.452	0.25	23.631	168.98	0.2068
38.4 1.625 x 3	1.625 x 3		1	22.034	0.2	31.508	173.56	0.2527
5.5 38.4 1.625 x 3	1.625 x 3		1	23.788	0.29	43.323	187.38	0.3182
38.4 1.625 x 3	1.625 x 3	_	1	22.5	0.24	821.38	177.23	0.383
38.4 1.625 x 3	1.625 x 3		1	24.284	0.29	63.015	191.28	0.4258
9.5 38.4 1.625 x 3	1.625 x 3	_	1	24.034	0.21	74.831	189.31	0.4879
38.4 1.625 x 3	1.625 x 3	_	I	24.444	0.27	96.646	192.54	0.5497
9.5 51.2 1.625 x 3	1.625 x 3		1	18.004	0.2	99.774	189.09	0.6185
10.5 51.2 1.625 x 3	1.625 x 3	-	1	10.01	0.23	110.277	199.65	0.6726
51.2 1.625 x 3	1.625 x	3	1	31.118	0.43	126.031	326.82	0.7324
		١						

the curve, while equation (20) is used to determine cumulative strain. The only problem at this point is knowing what initial stress value (buckling stress) to use for the variable σ_1 in equation (19) to calculate the change in strain for the 1st drop.

To find the buckling stress, the energy absorbed (sh/t) is plotted against dynamic stress, and a polynomial representing a "best fit" curve to the data is generated. Figure 17 shows the curve and polynomial which represents dynamic stress as a function of absorbed energy for edge crush cushions conditioned at 50% RH. The buckling stress is obtained by solving the polynomial when the energy absorbed by the cushion is zero. Simply stated, the constant term of the polynomial is an estimate of buckling stress, as the true value cannot be found. The buckling stress is expected to be less than the stress calculated for the first test condition (31.418), however, due to correlation error between the plotted data and the "best fit" curve, a value of 35.2961 is given as the constant. Thus, 31.418 was used as the buckling stress for the material. The change in strain then becomes:

$$\Delta \varepsilon = \frac{.875 - 0}{\left(\frac{31.418 + 31.418}{2}\right)} = .0279$$

The cumulative strain at this point is 0 + .0279 = .0279 according to equation (20). Repeating the process for the 2nd drop yields:

$$\Delta \varepsilon = \frac{2.626 - .875}{\left(\frac{31.418 + 83.385}{2}\right)} = .0305$$

The cumulative strain is .0279 + .0305 = .0584

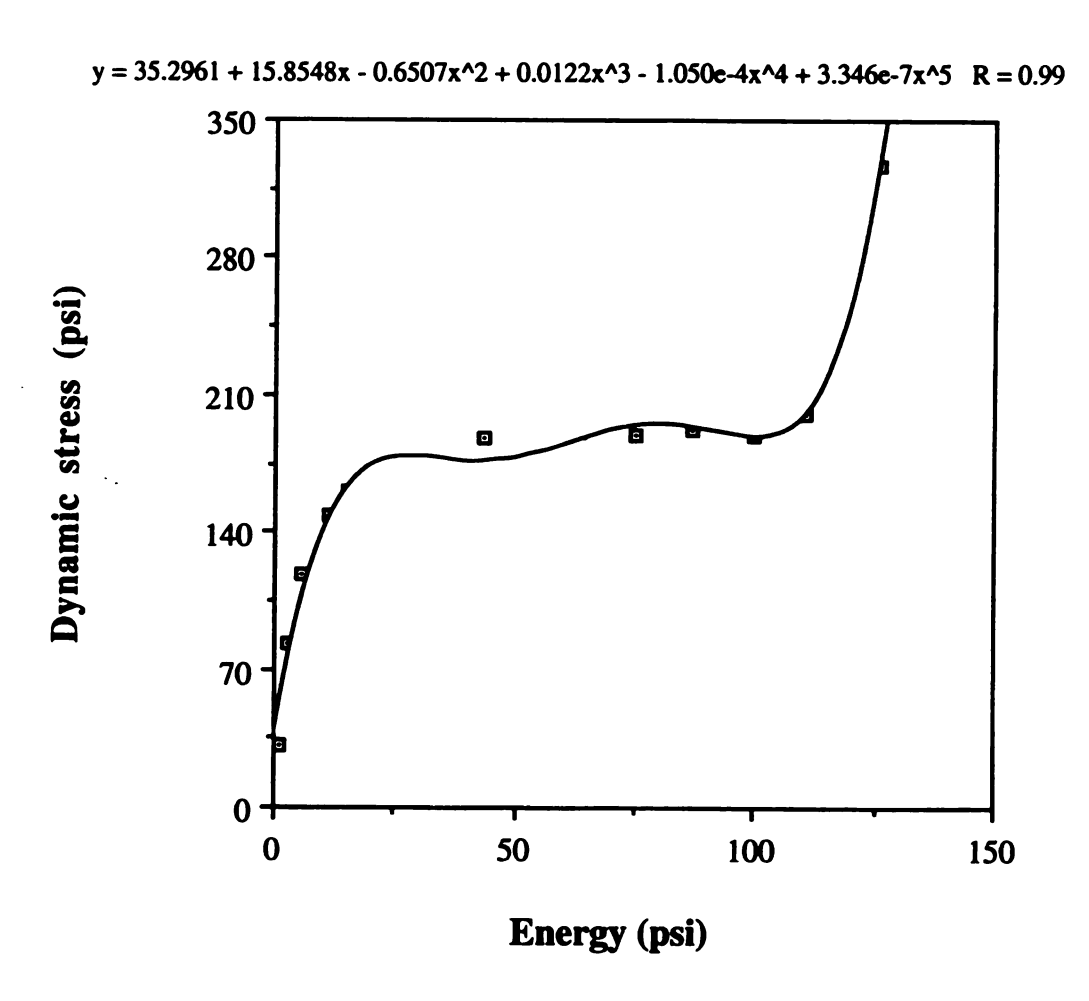


Figure 17: Dynamic stress vs. energy for C-flute in the edge crush mode @ 50% RH.

This process is repeated to find the remaining strains shown in Table 2. The absorbed energy is then plotted against the strain values and a polynomial representing dynamic strain as a function of energy absorbed is generated. This is shown in Figure 18. Finally, stress is plotted as a function of strain for the material.

The "working length" for a material can be estimated by inspecting the dynamic curve for the value of strain at which the stresses start to rapidly increase. Figure 19 shows the working length for edge cushions conditioned at 50% RH to be around 65%. In other words, an edge cushion can be compressed only 65% of its thickness before it starts to compact. The maximum useful energy absorption capacity for the material is taken to be the area under stress vs. strain curve up to this strain, and is estimated to be 110 psi for cushions in the edge crush mode.

Tables 3 and 4 show the energy vs. stress and strain relationships for the relative humidities shown in Table 1, and were calculated using equations (32) and (33). These relationships are important in determining the performance of corrugated cushions when they are exposed to extreme humidity conditions.

Predictions were made for drop conditions not used to generate the last three columns of Table 2 in order to test the accuracy of the model. Predictions were made for peak G, impact duration, and the number of useful drops. For example, consider the case where a 27.8 lb weight is dropped from 6" onto a $1.625" \times 2" \times 1"$ edge crush cushion. The static loading is 27.8/3.25 = 8.55

			i

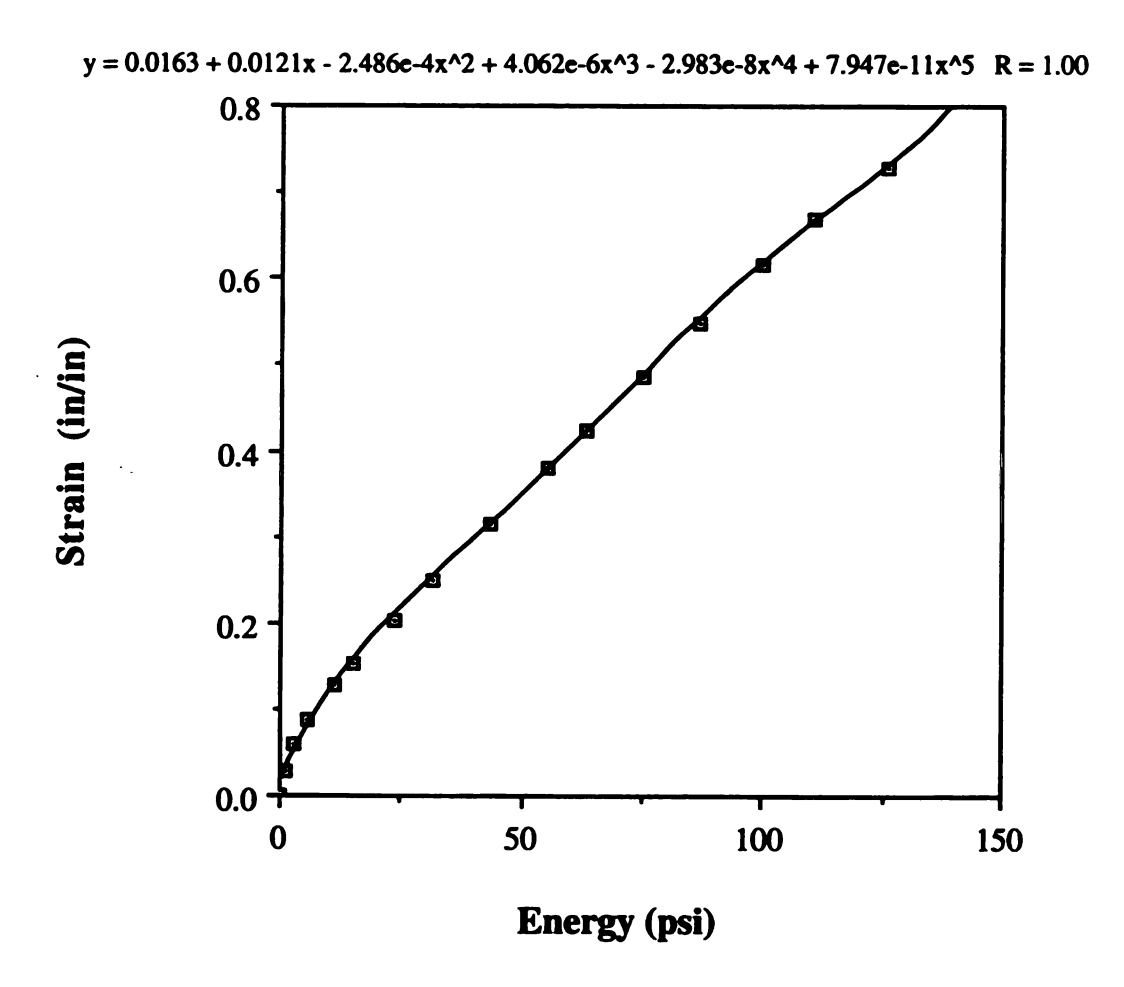


Figure 18: Dynamic strain vs. energy for C-flute in the edge crush mode @ 50% RH.

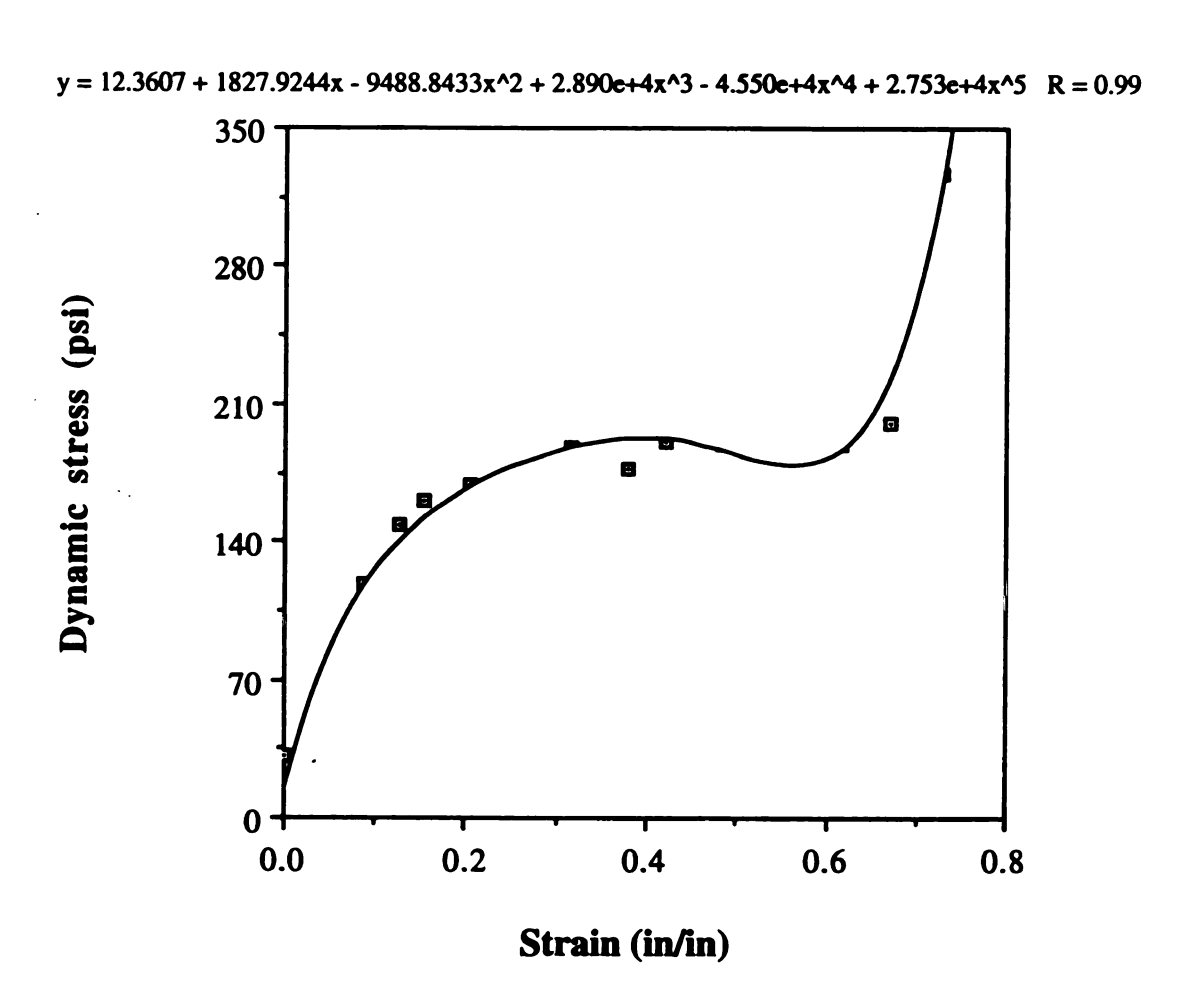


Figure 19: Dynamic stress vs. strain for C-flute in the edge crush mode @ 50% RH.

Table 3: Energy absorption versus dynamic stress data for C-flute in the edge crush mode at various humidity conditions.

Energy Absorbed	Stress	Stress	Stress	Stress	Stress	Stress
s*h/t (pst)	0% RH	25% RH	50% RH	75% RH	85% RH	90% RH
0.875	39.28	34.56	31.42	25.14	18.85	15.71
2.626	104.24	91.73	83.39	66.71	50.03	41.7
5.477	147.38	129.69	117.9	94.32	70.74	58.95
11.405	186.1	163.77	148.88	119.1	89.33	74.44
15.207	201.08	176.95	160.86	128.69	96.52	80.43
23.631	211.23	185.88	168.98	135.18	101.39	84.49
31.508	216.95	190.92	173.56	138.85	104.14	86.78
43.323	234.23	206.12	187.38	149.9	112.43	93.69
55.138	221.54	194.95	177.23	141.78	106.34	88.62
63.015	239.1	210.41	191.28	153.02	114.77	95.64
74.831	236.64	208.24	189.31	151.45	113.59	94.66
86.646	240.68	211.79	192.54	154.03	115.52	96.27
99.774	236.36	208	189.09	151.27	113.45	94.55
110.277	249.56	219.62	199.65	159.72	119.79	99.83
126.031	408.53	359.5	326.82	261.46	196.09	163.41

Table 4: Energy absorption versus dynamic strain data for C-flute in the edge crush mode at various humidity conditions.

Energy Absorbed	Strain	Strain	Strain	Strain	Strain	Strain
s*h/t (psi)	0% RH	25% RH	50% RH	75% RH	85% RH	90% RH
0.875	0.0223	0.0253	0.0279	0.0348	0.0464	0.0557
2.626	0.0467	0.053	0.0584	0.0729	0.0973	0.1167
5.477	0.0693	0.0788	0.0867	0.1084	0.1445	0.1734
11.405	0.1049	0.1192	0.1311	0.1639	0.2185	0.2623
15.207	0.1245	0.1415	0.1557	0.1946	0.2595	0.3113
23.631	0.1654	0.188	0.2068	0.2584	0.3446	0.4135
61.508	0.2022	0.2298	0.2527	0.3159	0.4212	0.5055
43.323	0.2546	0.2893	0.3182	0.3978	0.5304	0.6364
55.138	0.3064	0.3482	0.383	0.4788	0.6384	0.7661
63.015	0.3406	0.3871	0.4258	0.5322	0.7096	0.8516
74.831	0.3903	0.4435	0.4879	8609'0	0.8131	0.9757
86.646	0.4398	0.4998	0.5497	0.6872	0.9162	-
99.774	0.4948	0.5623	0.6185	0.7732	1	1
110.277	0.5381	0.6114	0.6726	0.8407	1	1
126.031	0.5859	0.6658	0.7324	0.9155	1	1

psi, and the energy absorbed by the cushion in the 1st drop is $27.8 \times 6/3.25 = 51.32$ psi.

- (1) Using either the graph or the polynomial in Figure (17) gives a corresponding dynamic stress of 174.93 psi and so the predicted peak G is 20.45 for the 1st drop.
- (2) Using an average value of .31 for the coefficient of restitution for edge crush cushions, the additional energy absorbed in the 2nd drop is $(1-.31^2)51.32 = 46.39$ psi. The total amount becomes 51.32 + 46.39 = 97.71 psi. From Figure (17) the corresponding stress is 162.27 psi and the predicted peak G is 18.97.
- (3) The total energy absorbed in the 3rd drop = 51.32 + 2(46.39) = 144.10 psi. The stress is 829.21 psi and the peak G is 96.94.

It can be deduced from above that the predicted number of useful drops for the cushion is two, as the energy to be absorbed exceeds the maximum capacity (110 psi) in the 3rd drop. Another way to find the number of useful drops is through equation (27),

$$N = 1 + \frac{1}{(1 - .31)} \left[\frac{110}{51.32} - 1 \right] = 2.66$$
 or just 2

To predict the impact duration for the 1st drop, the energy absorbed (51.32) is used in Figure 18 to find a strain value of .353, which corresponds to a dynamic compression of $.353 \times 1 = .353$ ". The predicted duration, in milliseconds is:

$$t_{dur} = \frac{4(.353)}{\sqrt{772.8 \times 6}} (1000) = 20.74 \text{ ms}$$

Predictions were made for seven different drop scenarios to check the accuracy of the above predictions. These conditions were then tested using actual edge crush cushions. Table 5 summarizes the results of those tests, and shows the comparison between the actual and predicted results.

As outlined in Chapter 2, energy vs. dynamic stress data can be used to generate conventional cushion curves, which relate drop parameters (drop height, cushion thickness, and static loading) to peak G. For example, suppose a set of cushion curves is to be made for edge crush cushions conditioned at 50% RH, and the selected drop height is 12". The chosen thicknesses are 1", 1.5", and 2". The first step is to set up the usual cushion curve axes by dividing the horizontal (static loading) and vertical (peak G) axes into suitable increments: 0 - 30 psi in steps of 5 psi, and 0 - 160 G's in steps of 20 G. To generate the curve for a thickness of 1", the energy absorbed values, $sh/t = s \times 12/1$, are calculated for each static loading on the horizontal axis. The corresponding stress values are obtained from Figure 17, and the peak G for these are plotted on the vertical axis. This process was repeated for the other thicknesses and the results are shown in Figure 20. Curves for other drop heights follow the same procedure. The rest of the cushion curves developed for C-flute edge crush cushions are summarized in Appendix B.

3.2 FLAT CRUSH DATA

Appendix C contains a portion of the shock pulses that were used to construct the energy absorbed vs. dynamic stress and strain data for flat

Table 5: Validation test for cushions in the edge crush mode conditioned @ 50% and 80% RH.

	Static	Drop			Peak G in drop	#of useful drops	Duration (ms)
Test #	Test # Loading (psi)	Height (in)	Thickness (in)	%RH	Predicted/Actual	Predicted/Actual	Predicted/Actual
1	7.88	9	1.5	90	22.51 / 22.59	3/2	20.67 / 16.17
2	11.82	13	1.5	20	13.35 / 17.99	1/1	36.44 / 30.00
3	4.68	4	1	20	36.77 / 30.66	119	11.69 / 12.33
4	8.55	9	1	20	20.45 / 21.53	2/2	20.73 / 17.17
5	7.88	9	1.5	80	15.89 / 18.93	3/2	29.77 / 19.67
9	4.68	4	1	80	26.02 / 26.43	119	16.73 / 13.50
7	8.55	9	1	80	14.34 / 17.88	2/1	28.41 / 20.00

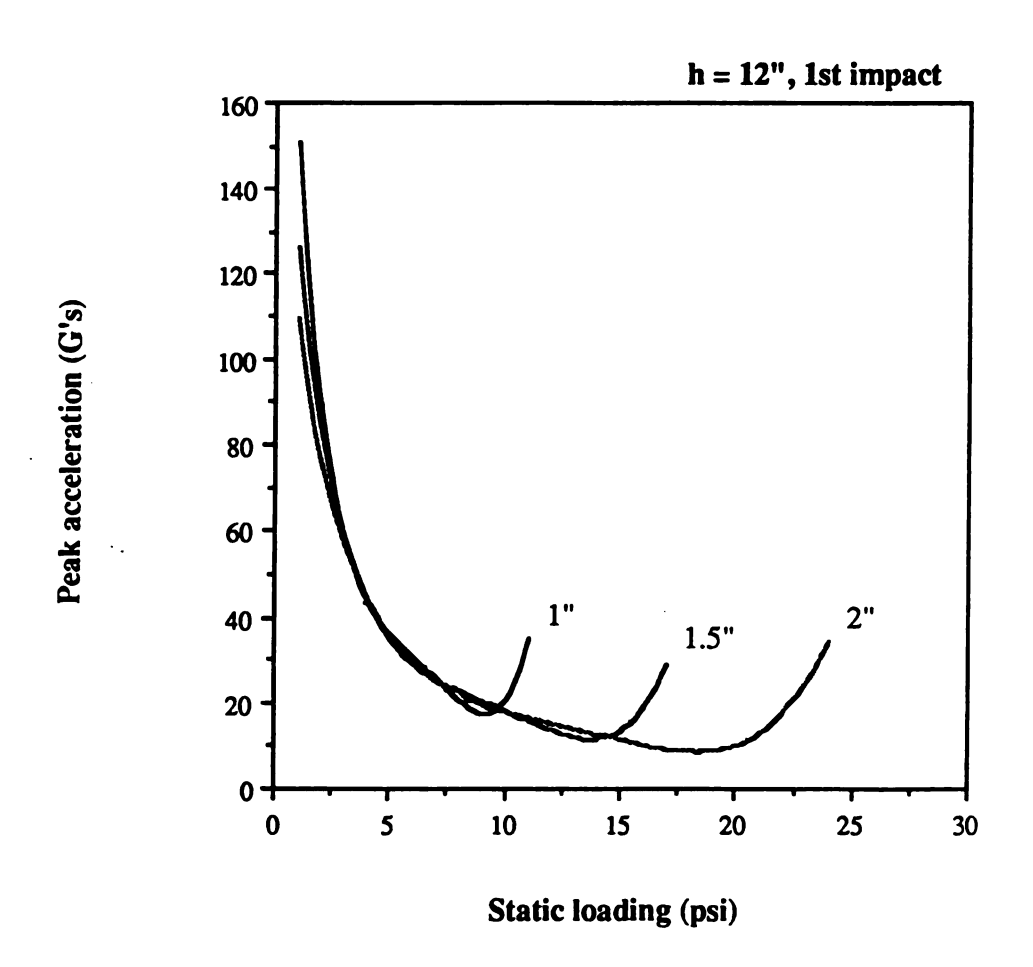


Figure 20: Cushion curve for 12" drop for C-flute board in edge crush mode @ 50% RH.

crush cushions shown in Table 6. It's important to reiterate that the data in the first six columns of the table relate only to the specific drop parameters and cushion sizes tested, but the last three columns describe a property of the material which can be applied to any drop situation, provided the cushions are conditioned to the same humidity conditions (50% RH). As with edge crush cushions, dynamic stress was plotted against absorbed energy, and a "best fit" polynomial was generated. This is shown in Figure 21. The dynamic strain values were calculated using equations (19) and (20). The stress of 4.9381 psi from the fitted polynomial was used as the buckling stress. Next, strain was plotted against energy absorbed, as shown in Figure 22, so that dynamic compression data could be calculated. Finally, stress was plotted as a function of strain so that the working length for flat crush cushions could be obtained by visual inspection. The resulting curve and polynomial is shown Figure 23. The area under the curve up to the working length strain represents the amount of energy the cushion can absorb before bottoming out. For flat cushions, the energy absorption capacity is approximately 9 psi. Tables 7 and 8 describe the energy absorbed vs. dynamic stress and strain relationships for flat cushions over a wide range of humidity conditions.

Six different drops were performed to test the accuracy of the prediction formulas; none of these drops replicated those used to construct the original data in Table 6. The results of the test are shown in Table 9. The method of analysis was identical to that performed for edge crush cushions.

The energy absorbed vs. dynamic stress columns from Table 6, along with equations (31) and (32) were used to produce conventional cushion curves

Table 6: Dynamic stress and strain versus energy absorption data for C-flute in the flat crush mode @ 50%RH.

Drop		Cushion		Peak G		Energy Absorbed	Stress	Strain
Height (in)	Weight (lb)	Area (sq. in.)	Thickness (in)	in drop	ð	s*h/t (psi)	G*s (psi)	(in/in)
2	12.8	6.5 x 6.5	1.625	31.794	0.83	0.373	9.63	0.0512
4	12.8	6.5 x 6.5	1.625	39.678	0.74	97.0		0.0857
9	12.8	6.5 x 6.5	1.625	42.28	9.0	1.119	12.81	0.1157
9	16.6	6.5 x 6.5	1.625	35.128	0.57	1.451	13.8	0.1407
9	21.6	6.5 x 6.5	1.625	28.16	0.54	1.888	14.4	0.1717
9	25.6	6.5 x 6.5	1.625	24.524	0.54	2.237	14.86	0.1955
•	29.4	6.5 x 6.5	1.625	22.76	0.49	2.569	15.84	0.2171
9	20.4	5 x S	1.625	19.292	0.45	3.013	15.74	0.2453
9	22.95	5 x S	1.625	18.324	0.48	3.39	16.82	0.2684
9	25.6	5 x S	1.625	16.342	0.48	3.781	16.73	0.2917
9	28.15	5 x S	1.625	14.856	0.44	4.158		0.3143
9	30.7	5 x S	1.625	14.688	0.46	4.534	18.04	0.3359
9	21.6	4×4	1.625	13.072	0.52	4.985	17.65	0.3612
10	15.35	4×4	1.625	17.608	0.43	2.904	16.89	0.4144
10	17.8	4×4	1.625	15.362	0.38	98.9	17.1	0.4698
10	20.35	4 x 4	1.625	15.086	0.38	7.827	19.19	0.5239
10	21.65	4×4	1.625	14.128	0.37	8.327	19.12	0.55
10	24.2	4×4	1.625	16.758	0.37	806.6	25.35	0.5941
10	26.9	4×4	1.625	22.148	0.44	10.346	37.24	0.6272
10	29.4	4×4	1.625	28.996	0.52	11.308	53.28	0.6485
10	31.95	4×4	1.625	36.222	0.46	12.288	72.33	0.6641
10	34.4	4 x 4	1.625	39.476	0.49	13.231	84.87	0.6761
10	38.4	4×4	1.625	46.214	0.54	14.769	16'011	0.6918
10	42.2	4×4	1.625	48.568	0.51	16.231	128.1	0.7041
10	47.2	4 x 4	1.625	54.84	0.49	18.154	161.78	0.7173

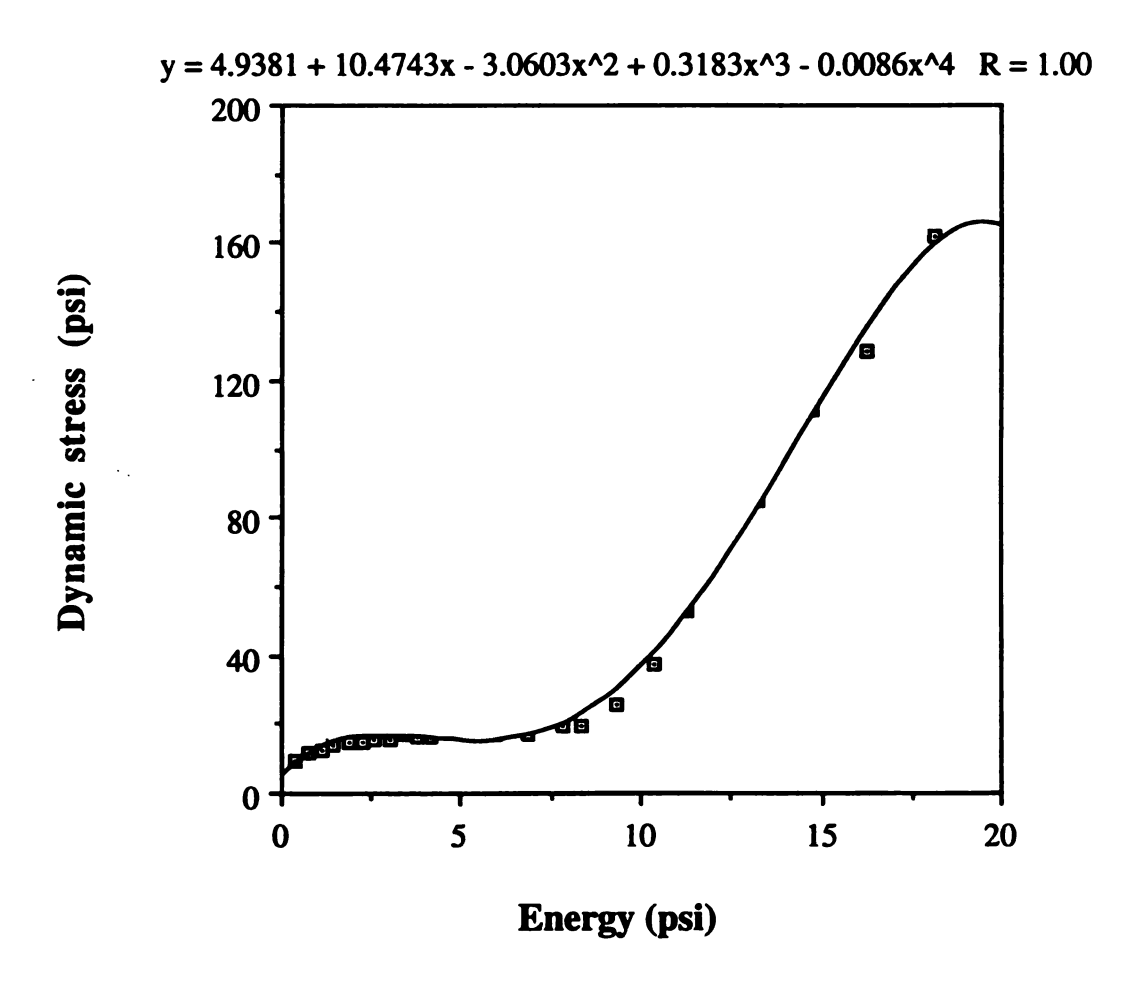


Figure 21: Dynamic stress vs. energy for C-flute in flat crush mode @ 50% RH.

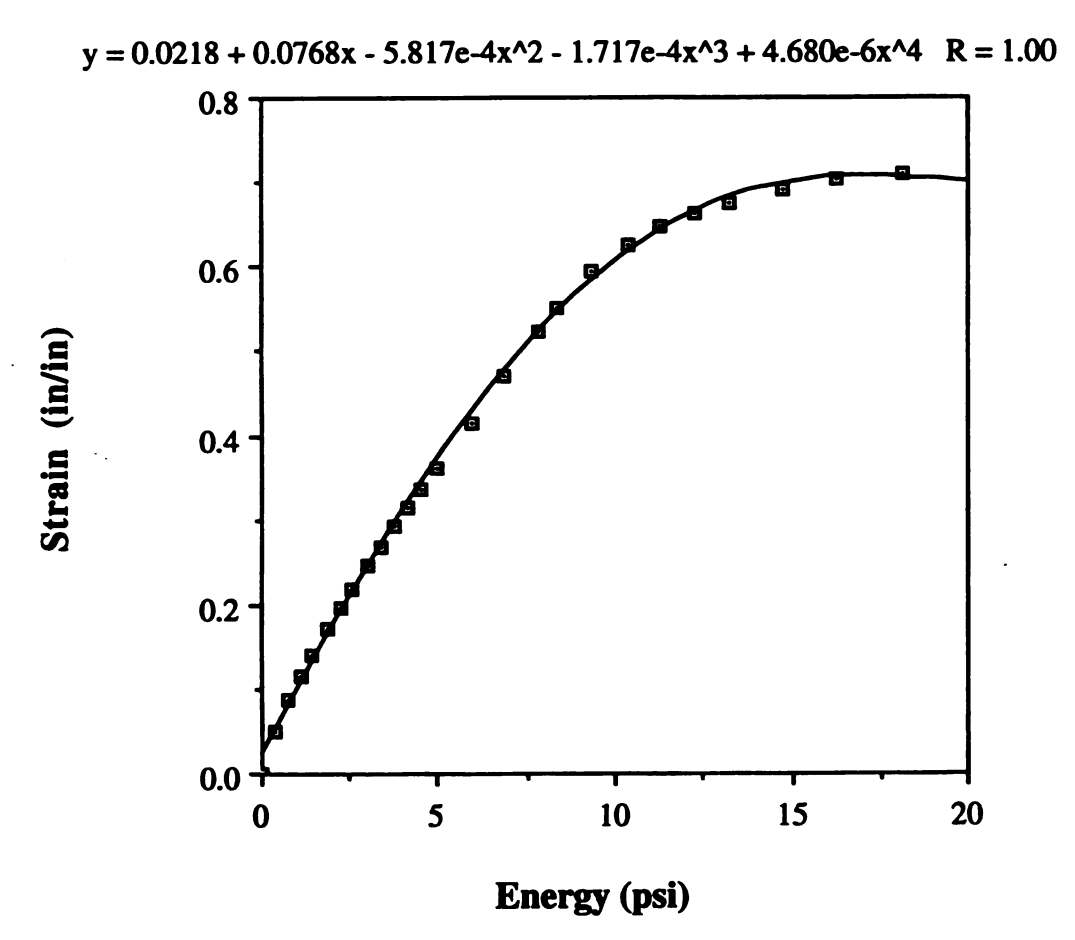


Figure 22: Dynamic strain vs. energy for C-flute in flat crush mode @ 50% RH.

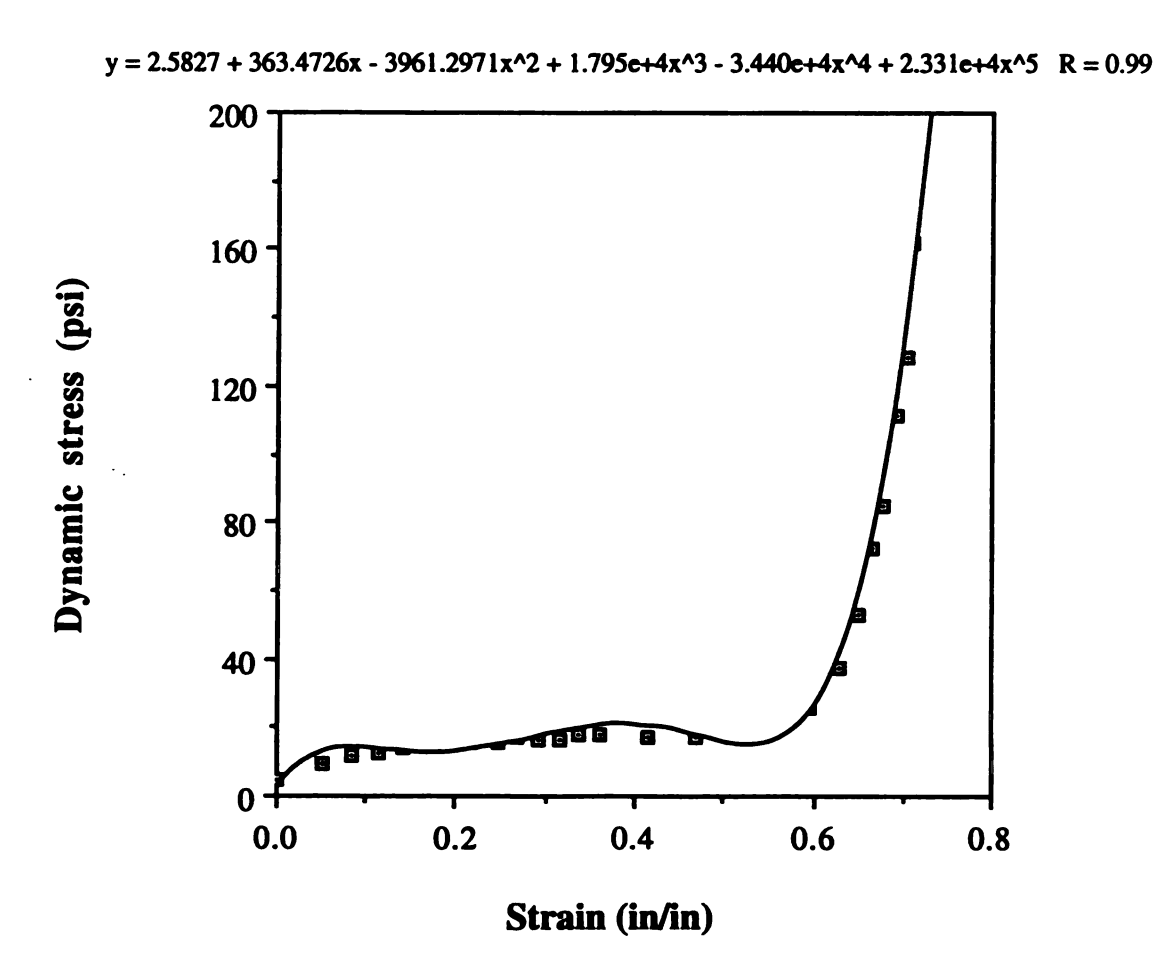


Figure 23: Dynamic stress vs. strain for C-flute in flat crush mode @ 50% RH.

Table 7: Energy absorption versus dynamic stress data for C-flute in the flat crush mode at various humidity conditions.

Energy Absorbed	Stress	Stress	Stress	Stress	Stress	Stress
	0% RH	25% RH	50% RH	75% RH	85% RH	90% RH
0.373	12.04	10.59	9.63	1.7	5.78	4.82
0.746	15.03	13.22	12.02	9.62	7.21	6.01
1.119	16.01	14.09	12.81	10.25	69'L	6.41
1.451	17.25	15.18	13.8	11.04	8.28	6.9
1.888	18	15.84	14.4	11.52	8.64	7.2
2.237	18.58	16.35	14.86	11.89	8.92	7.43
2.569	19.8	17.42	15.84	12.67	9.5	7.92
3.013	19.68	17.31	15.74	12.59	9.44	7.87
3.39	21.03	18.5	16.82	13.46	10.09	8.41
3.781	20.91	18.4	16.73	13.38	10.04	8.37
4.158	20.91	18.4	16.73	13.38	10.04	8.37
4.534	22.55	19.84	18.04	14.43	10.82	9.02
4.985	22.06	19.42	17.65	14.12	10.59	8.83
5.904	21.11	18.58	16.89	13.51	10.13	8.45
6.846	21.38	18.81	17.1	13.68	10.26	8.55
7.827	23.99	21.11	19.19	15.35	11.51	9.6
8.327	23.9	21.03	19.12	15.3	11.47	9.56
9.308	31.69	27.89	25.35	20.28	15.21	12.68
10.346	46.55	40.96	37.24	29.79	22.34	18.62
11.308	9.99	58.61	53.28	42.62	31.97	26.64
12.288	90.41	79.56	72.33	57.86	43.4	36.17
13.231	106.09	93.36	84.87	6.79	50.92	42.44
14.769	138.64	122	110.91	88.73	66.55	55.46
16.231	160.13	140.91	128.1	102.48	76.86	64.05
18.154	202.23	177.96	161.78	129.42	97.07	80.89

Table 8: Energy absorption versus dynamic strain data for C-flute in the flat crush mode at various humidity conditions.

Energy Absorbed	Strain	Strain	Strain	Strain	Strain	Strain
s*h/t (pst)	0% RH	25% RH	50% RH	75% RH	85% RH	90% RH
0.373	0.041	0.0466	0.0512	0.064	0.0853	0.1024
0.746	0.0685	0.0779	0.0857	0.1071	0.1428	0.1713
1.119	0.0926	0.1052	0.1157	0.1446	0.1928	0.2314
1.451	0.1125	0.1279	0.1407	0.1758	0.2344	0.2813
1.888	0.1373	0.1561	0.1717	0.2146	0.2861	0.3433
2.237	0.1564	0.1777	0.1955	0.2444	0.3259	0.391
2.569	0.1737	0.1974	0.2171	0.2714	0.3619	0.4343
3.013	0.1962	0.223	0.2453	0.3066	0.4088	0.4905
3.39	0.2147	0.244	0.2684	0.3355	0.4474	0.5368
3.781	0.2334	0.2652	0.2917	0.3647	0.4862	0.5834
4.158	0.2514	0.2857	0.3143	0.3928	0.5238	0.6285
4.534	0.2687	0.3054	0.3359	0.4199	0.5598	0.6718
4.985	0.2889	0.3283	0.3612	0.4514	0.6019	0.7223
5.904	0.3315	0.3767	0.4144	0.518	0.6906	0.8287
6.846	0.3758	0.4271	0.4698	0.5873	0.783	0.9396
7.827	0.4191	0.4762	0.5239	0.6548	0.8731	1
8.327	0.44	0.5	0.55	0.6874	0.9166	1
9.308	0.4753	0.5401	0.5941	0.7426	0.9901	1
10.346	0.5018	0.5702	0.6272	0.7841	1	1
11.308	0.5188	0.5896	0.6485	0.8106	1	1
12.288	0.5313	0.6037	0.6641	0.8301	1	1
13.231	0.5409	0.6146	0.6761	0.8451	1	1
14.769	0.5535	0.6289	0.6918	0.8648	1	
16.231	0.5632	0.6401	0.7041	0.8801	1	1
18.154	0.5739	0.6521	0.7173	0.8967	I	1

Table 9: Validation test for cushions in the flat crush mode conditioned @ 50% and 80% RH.

	Static	Drop			Peak G in drop	#of useful drops	Duration (ms)
Test#	Loading (psi)	Height (in)	Thickness (in)	%RH	Thickness (in) %RH Predicted/Actual	Predicted/Actual	Predicted/Actual
1	1.42	5	0.8125	20	17.65 / 15.13	1/1	29.60 / 27.00
2	2.4	10	1.625	50	45.15 / 47.30	0/0	51.67 / 22.30
3	0.8	5	1.625	20	20.76 / 16.72	5/7	19.13 / 26.00
4	0.5	8	0.8125	20	30.93 / 26.75	2/2	14.17 / 19.17
5	0.5	8	0.8125	80	14.53 / 14.56	7/7	30.33 / 27.33
9	0.8	5	1.625	80	21.68 / 23.98	315	20.53 / 22.00

for C-flute corrugated cushions in the flat crush mode. The same process that was used to develop the impact data for edge crush cushions was used to generate the curves for the 1", 2", and 3" flat crush cushions shown in Figure 24. The rest of the cushion curves developed for flat crush cushions are summarized in Appendix D.

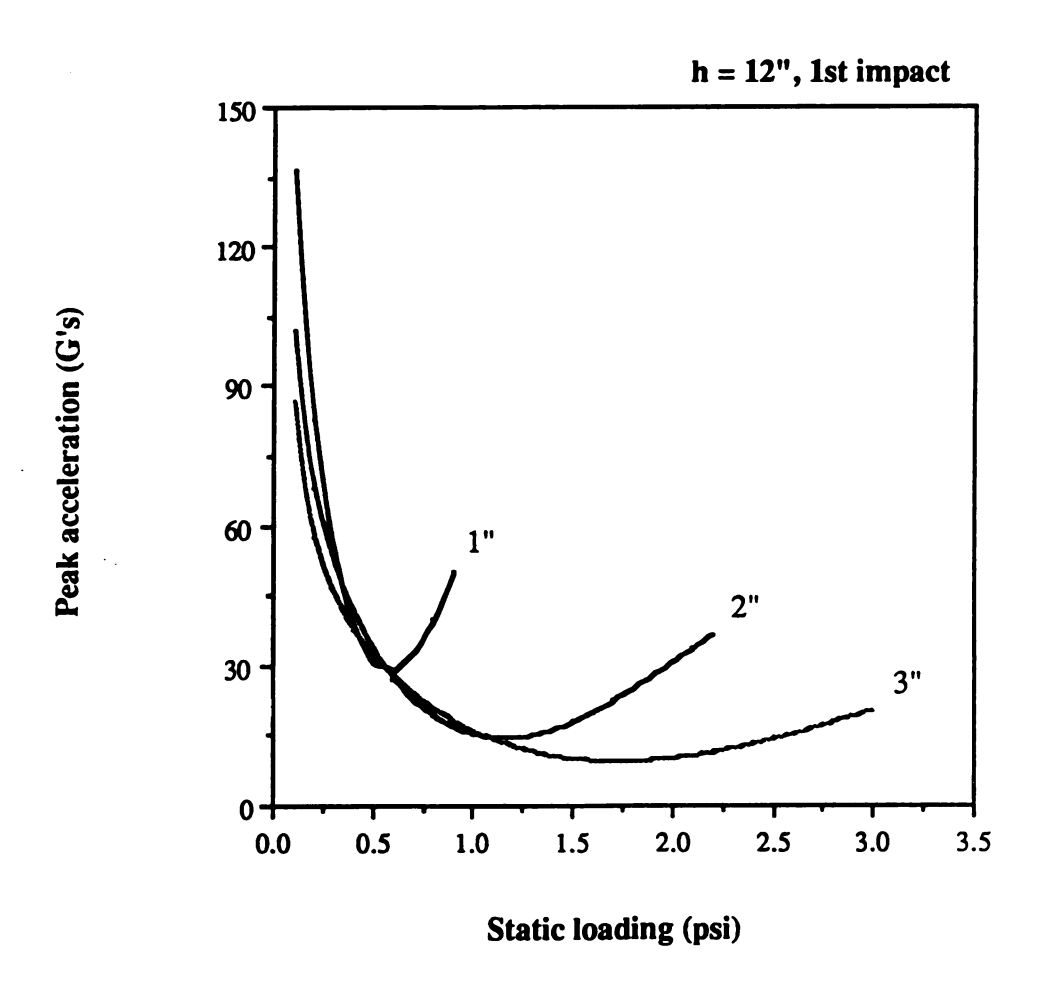


Figure 24: Cushion curve for 12" drop for C-flute board in flat crush mode @ 50% RH.

CHAPTER 4

DISCUSSION AND CONCLUSIONS

4.1 UTILITY OF METHOD

There are several advantages to the energy vs. stress method outlined in this study over using conventional cushion curves. First, the number of drops required to produce conventional curves for a cushioning material can be immense. For example, to obtain impact data for seven different drop heights, six static loadings, and for five cushion thicknesses at five repetitions per condition requires $7 \times 6 \times 5 \times 5 = 1050$ drops to be made. Hence, a large collection of these curves are required for a reasonably complete description of performance for a material, and this only provides data for a limited number of drop scenarios. By utilizing the procedure developed in this study, drop parameters are combined into two important energy absorbed and dynamic stress. Fortunately, the quantities: relationship between these quantities is obtainable from a small number of drops, and the results may be applied over a continuous range of drop heights and thicknesses. In addition, the energy vs. strain relationship provides a method for calculating dynamic compression data, where cushion curves do not. The working length, and the number of useful drops for partially elastic materials may also be estimated. Lastly, use of this method to generate conventional cushion curves drastically reduces the amount of lab time spent in developing such data.

4.2 EXPERIMENTAL ERRORS

There were several possible sources of error associated with this experiment that may have affected the results. The most obvious is the variability of corrugated fiberboard itself. Any crushing or damage to the material prior to drop testing may have affected the results. Since the cushions were manually constructed, imperfect cuts in the individual layers, or inconsistent amounts of spray adhesive between the layers could affect the data. Another source of error is the signal error from the accelerometer and Testpartner. The error in peak G associated with the accelerometer and coupler are $\pm 2\%$ and $\pm 5\%$ respectively. Other contributing factors include accelerometer calibration, triboelectric noise, transverse acceleration response, and ringing of the fixture. Due to the large amount of noise superimposed on the underlying shock pulses, choosing the correct filter frequency was crucial because it greatly affected the peak G reported by Testpartner. Figures 25 and 26 illustrate that reported peak G may disagree by more that 100% between filtered and unfiltered shock pulses.

Error may also originate from the curve fitting software that was used to generate polynomials representing the plotted data. Although the correlations between the plotted data and the "best fit" curves were excellent, they were not perfect.

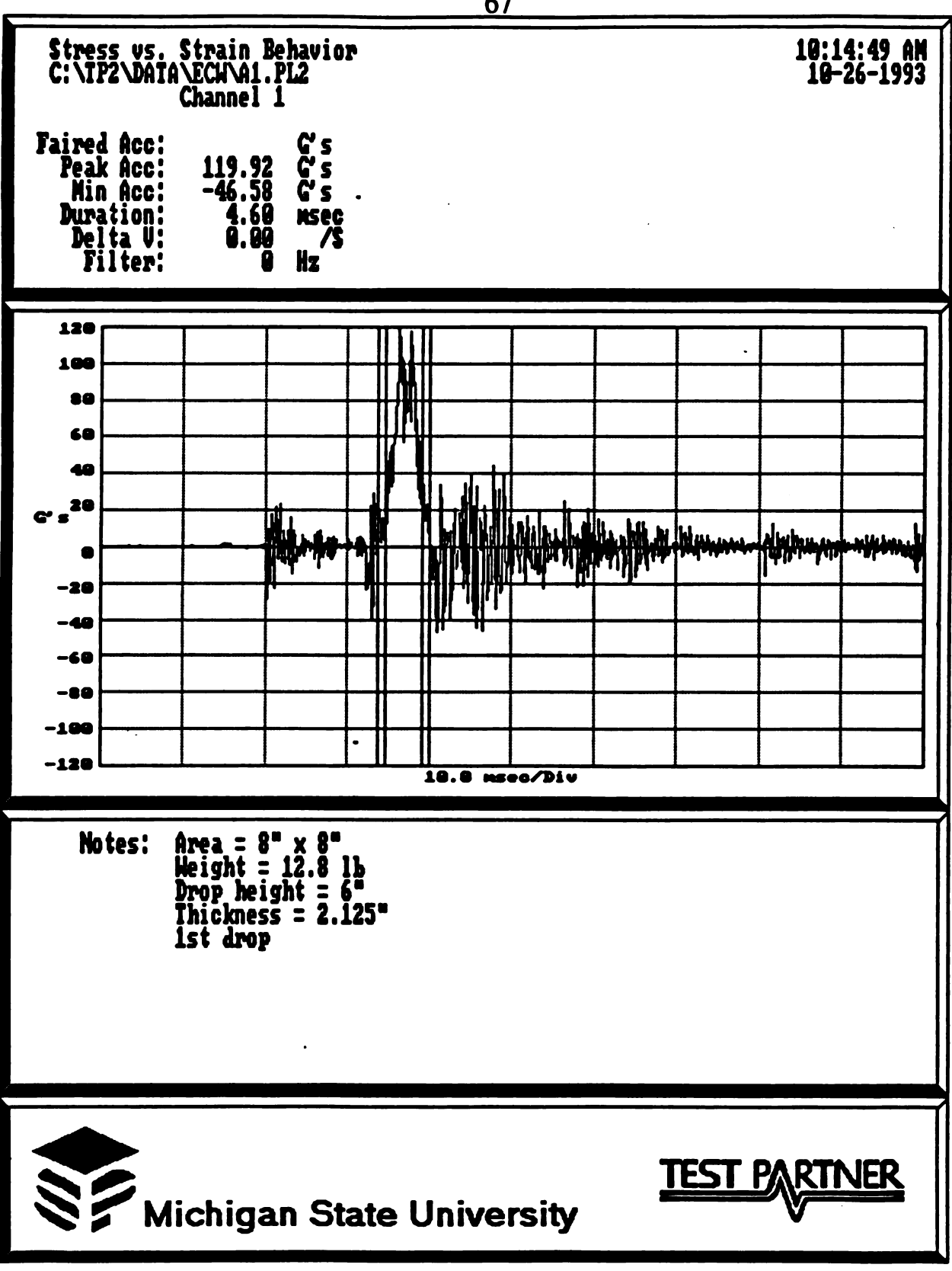


Figure 25: Unfiltered shock waveform.

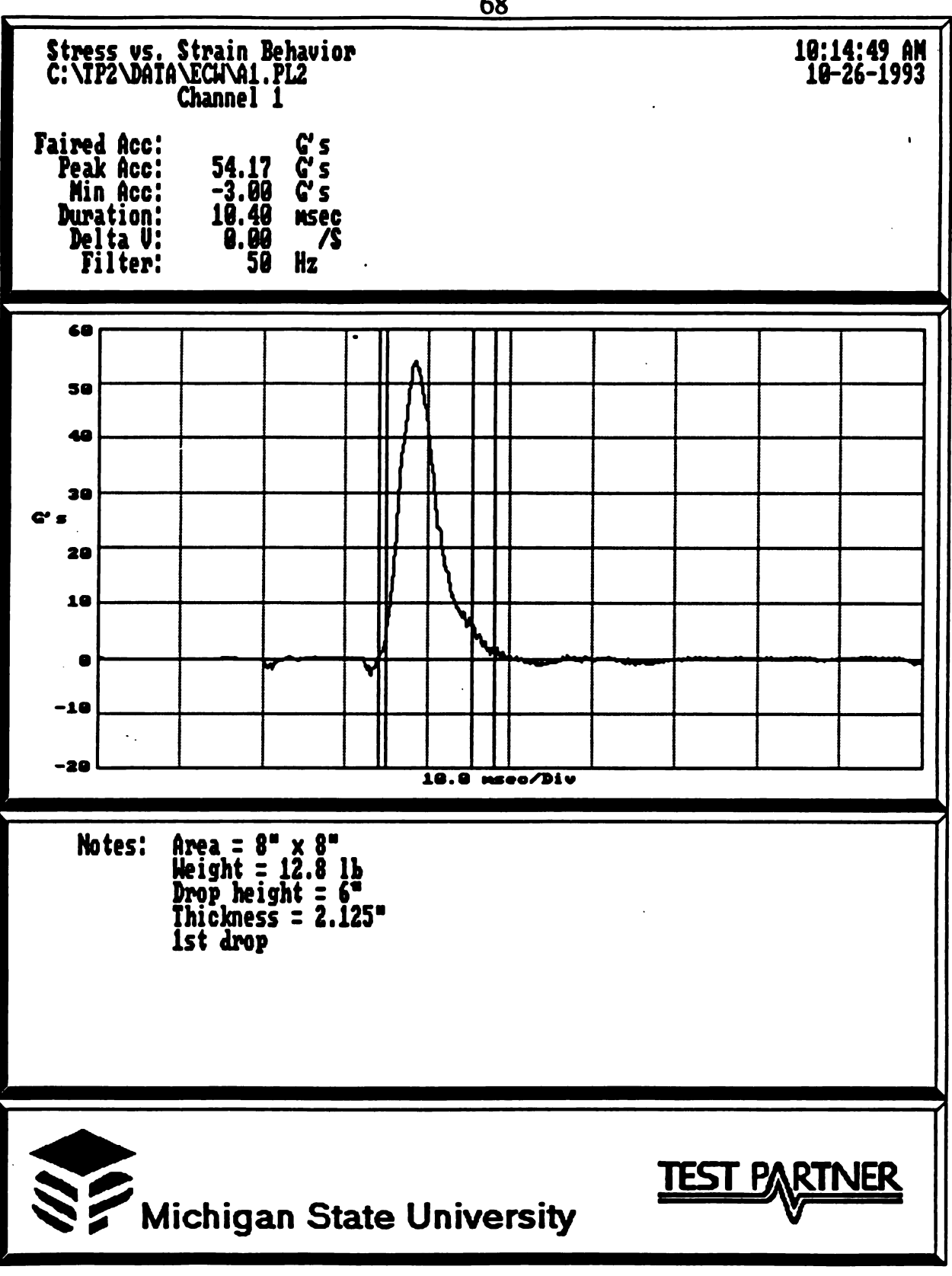


Figure 26: Filtered shock waveform.

4.4 ANALYSIS OF RESULTS

The validation tests which were used to check the accuracy of the prediction formulas produced results which were in excellent agreement for both peak G and the number of useful drops for both flat and edge crush cushions. The average percent error for peak G was around 14.5% for edge cushions and 10.5% for flat cushions. The predictions made for impact durations were not as accurate, as the average percent error was 20.7% for edge crush cushions and 22.5% for flat crush cushions.

There are several factors which contribute to the error in the duration predictions. The first is that the durations reported by Testpartner are based on the method outlined in ASTM 3332 [16], which defines the duration to be the time span between points on a shock pulse corresponding to 10% of the peak acceleration. The prediction formula developed for this study predicts true impact duration (i.e. the time span between G = 0 to G = 0). Hence, it was necessary to estimate the duration of the shock pulses by visual inspection rather than rely on Testpartner to do the comparison. Second, the prediction formula assumes a constant deceleration over the duration of the impact when this is clearly not the case. To develop a prediction which accounts for the non-constant deceleration is very complicated, and is beyond the scope of this work.

The agreement between the predicted and actual number of useful drops was excellent, as no test disagreed by more than one drop even though average values for the coefficient of restitution were used in equation (27).

4.5 COMPARING WITH OTHER CUSHIONING MATERIALS

Table 10 compares the performance of C-flute corrugated board to two other cushioning materials by examining the peak G level for six different drop scenarios. Inspection of this data reveals some very important characteristics of corrugated cushions. When the cushions are forced to absorb a small amount of energy (#1, 2), corrugated cushions in the flat crush mode outperform the others. The edge crush cushions produce the highest peak G for these drop conditions. When cushions absorb a medium amount of energy (#3, 4), both the Arpro 3313 [17] and the Arcel 310 [18] show better performance. For high energy absorption impacts, (#5, 6) the flat crush mode cushions bottom out as they have exceeded their energy absorbing capacity. The edge cushions provide the best protection for single drops at these conditions.

In conclusion, corrugated cushions provide excellent protection for items that are subjected to a limited number of drops. Flat crush cushions are best suited for lightweight items, while edge crush cushions, which are much stiffer, are best suited for heavy items. In order to use corrugated as a cushioning material, a reasonably accurate assessment of the distribution environment is required so as to ensure the average number of impacts does not exceed the maximum energy capacity of the material. Corrugated board is cheap to produce compared to the cost of fabricating foam cushions, and can easily be separated from other materials. Hence, it is easily recycled.

Table 10: Comparing the performance of corrugated board to other cushioning materials.

	Static	Drop			Peak G - 1st impact	mpact	
Test#	Fest # Loading (psi)	Height (in)	Thickness (in)	Flat cushion	Edge cushion	Arpro 3313	Arcel 310
1	0.5	36	3	30.40		41	38
2	3	12	7	6	43.20	6	7
3	2	18	3	30.80	73.50	18	17
4	2	18	7	0 <i>L'LL</i>	83.40	LZ	20
5	2	24	2	N/A	86.80	45	27
9	5	24	2	W/N	35	Y/N	A/A

4.6 FUTURE WORK

The cushions used to develop the energy absorbed vs. dynamic stress and strain data were constructed from C-flute corrugated fiberboard. It is expected, however that the performance of cushions made from different board will vary as a result of flute geometry, number of flutes per foot, and basis weight combinations characteristic of each board. Initial tests performed on cushions made of different flutes have shown results which vary widely. It is reasonable to expect that the dynamic stress vs. strain curve for B-flute for example, will relate to the C-flute curve by:

$$\sigma[B-flute] = C \times \sigma[C-flute]$$
 (35)

In other words, the stresses are simply scaled by some constant C. The value of the constant will most likely originate from one of the following relationships existing between the boards:

- (a) A ratio of the flat or edge crush values.
- (b) A ratio of the number of flutes per foot.

Another area which may be investigated is to develop a method for predicting peak G for dynamic drops made with ribbed corrugated cushions.



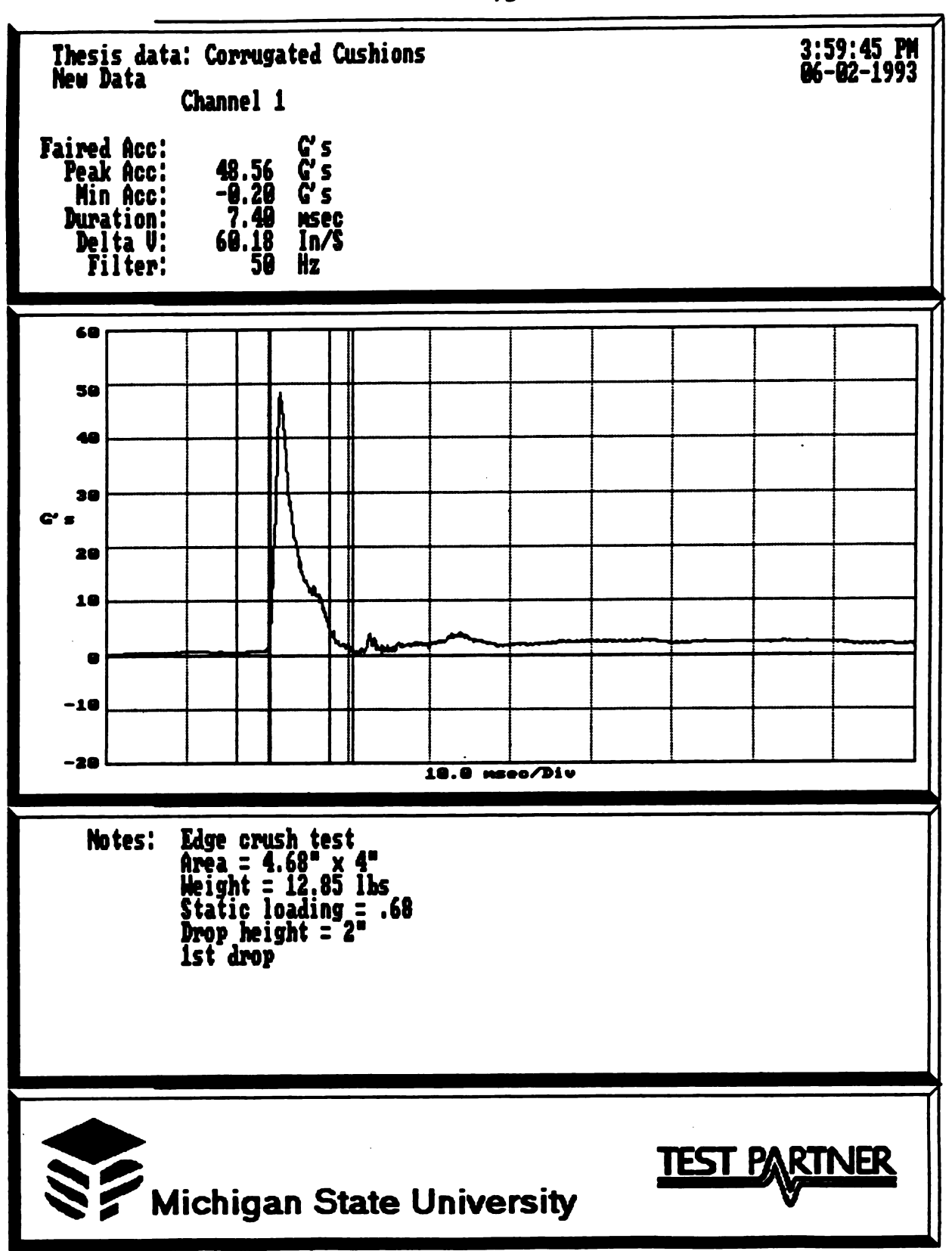


Figure 27: Shock pulse from edge cushion subjected to 1st drop conditions.

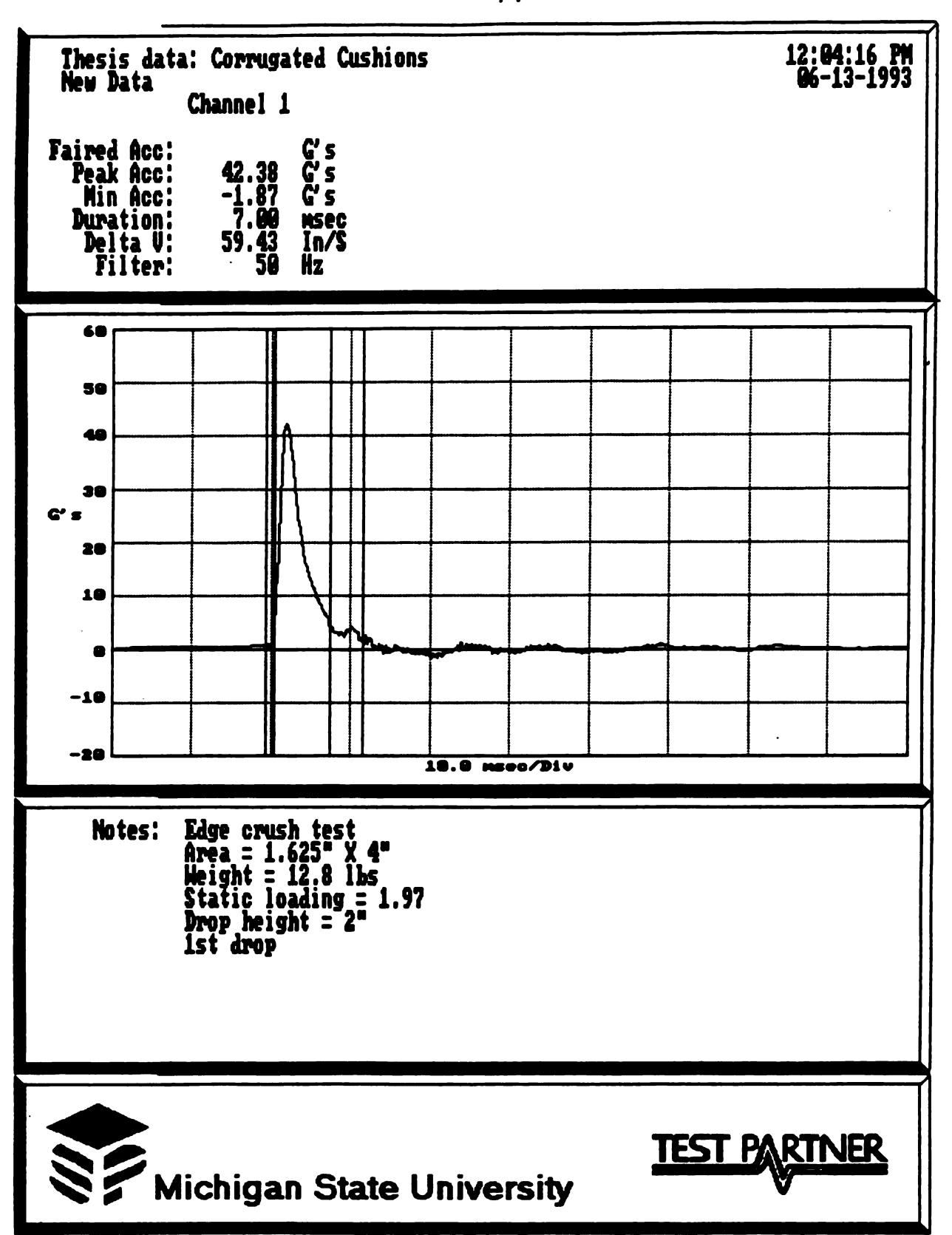


Figure 28: Shock pulse from edge cushion subjected to 2nd drop conditions.

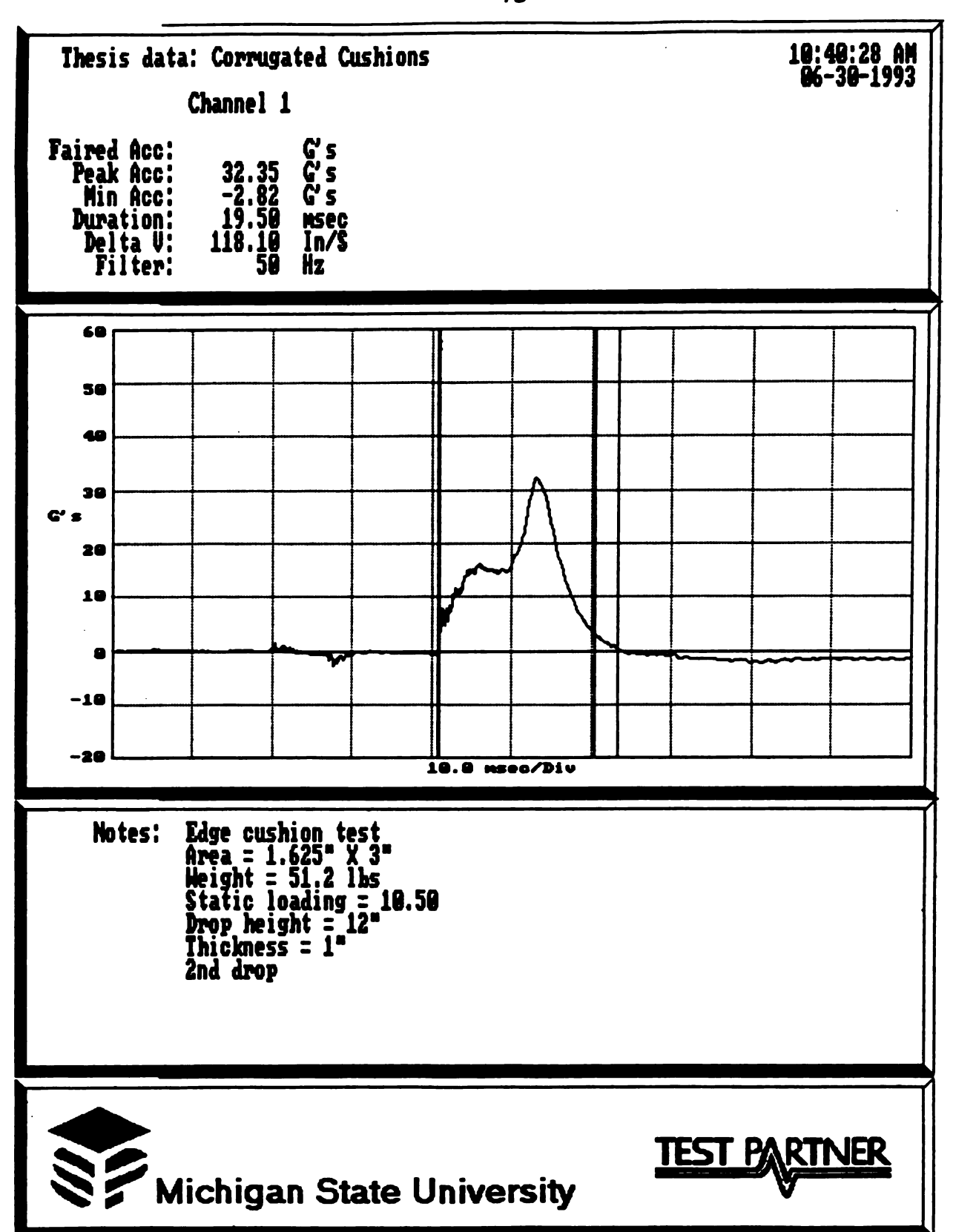
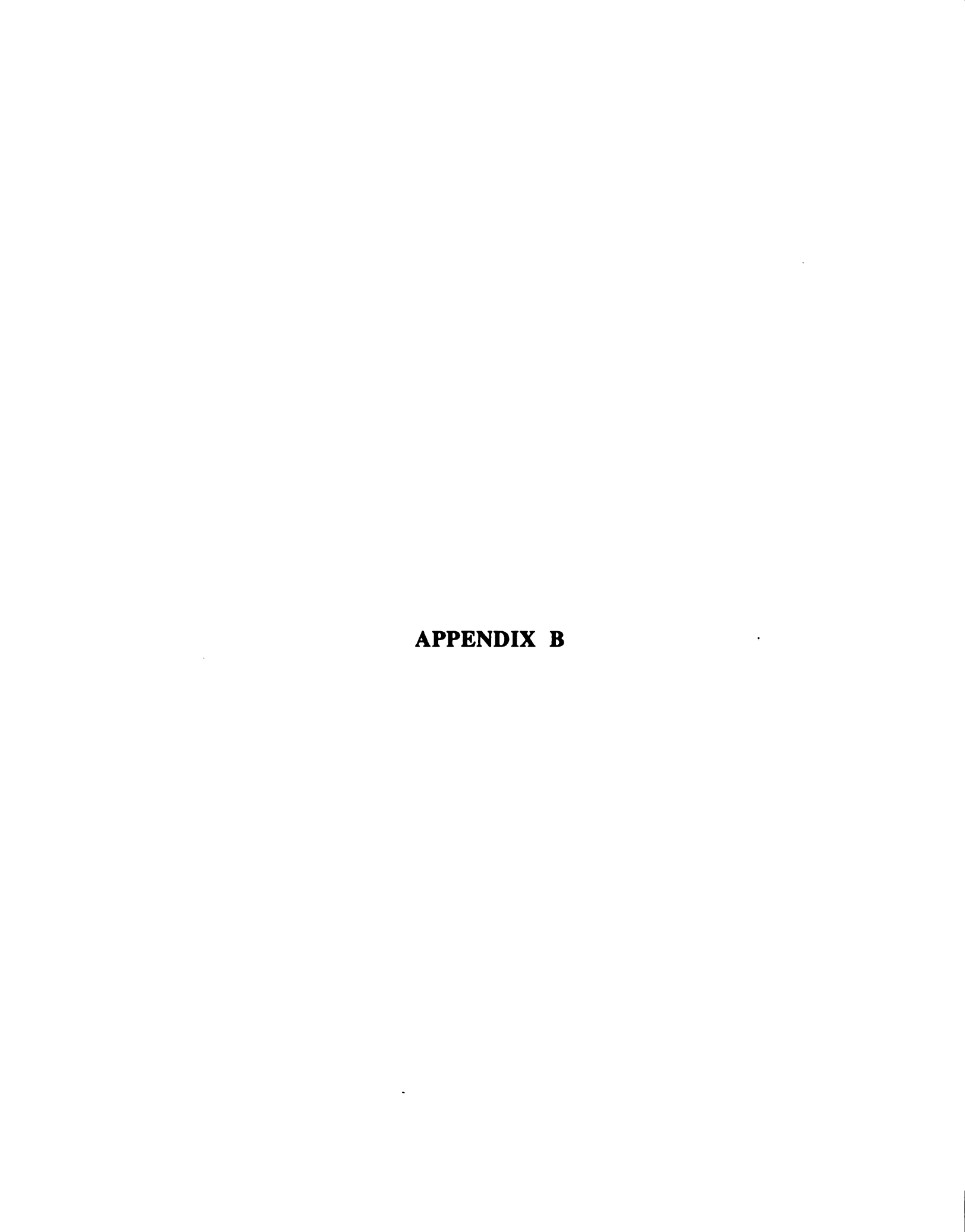


Figure 29: Shock pulse from edge cushion subjected to last drop conditions.



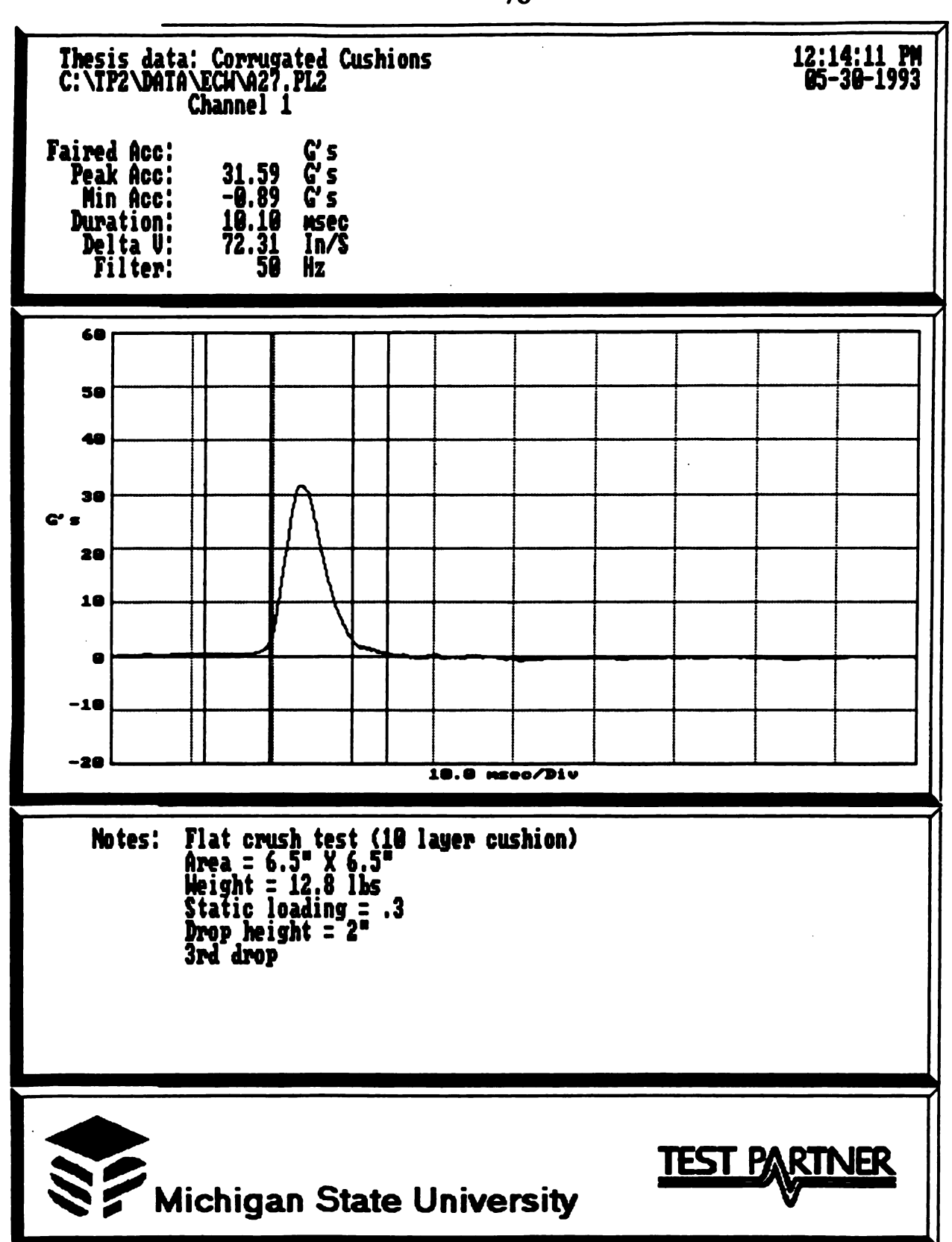


Figure 30: Shock pulse from flat cushion subjected to 1st drop conditions.

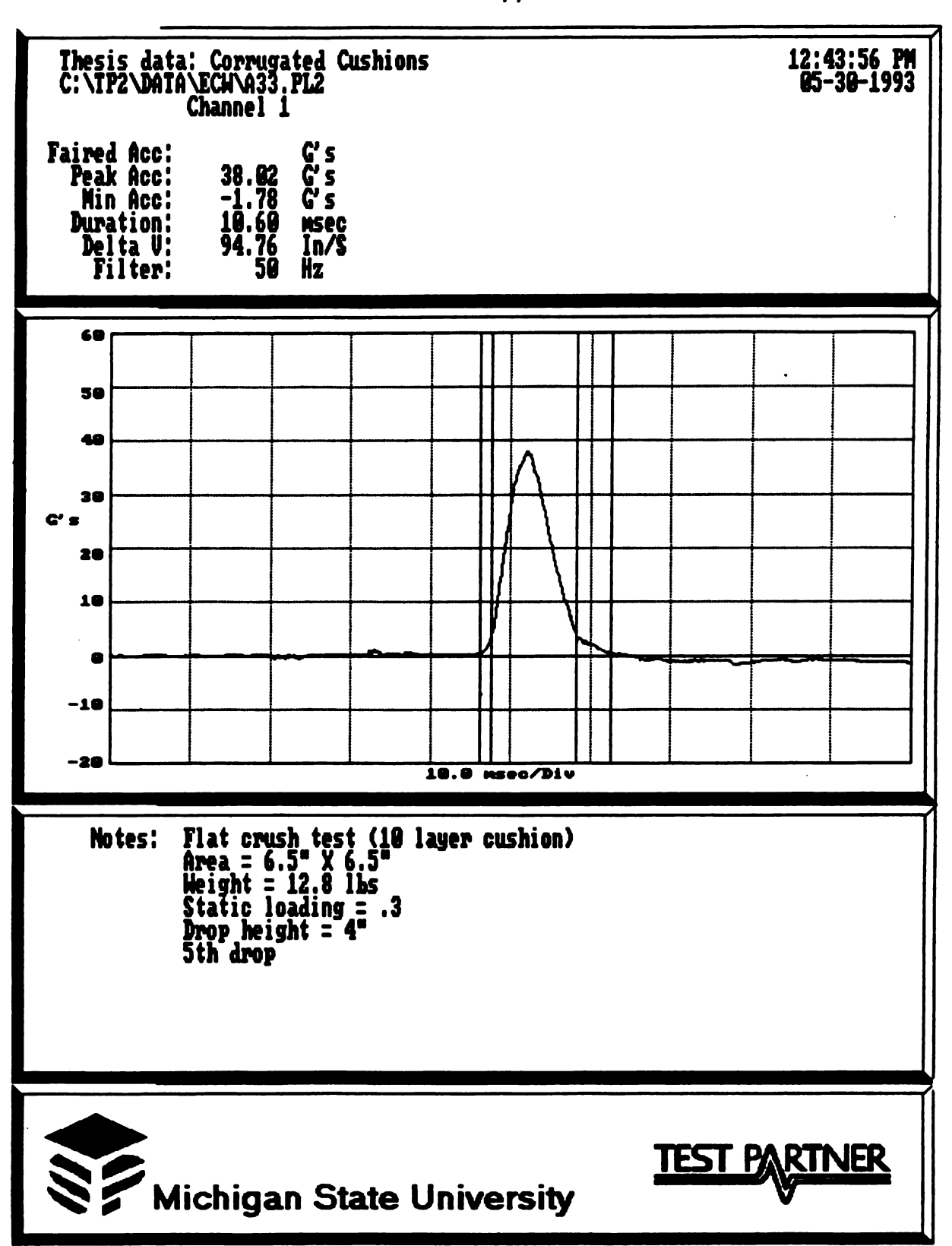


Figure 31: Shock pulse from flat cushion subjected to 2nd drop conditions.

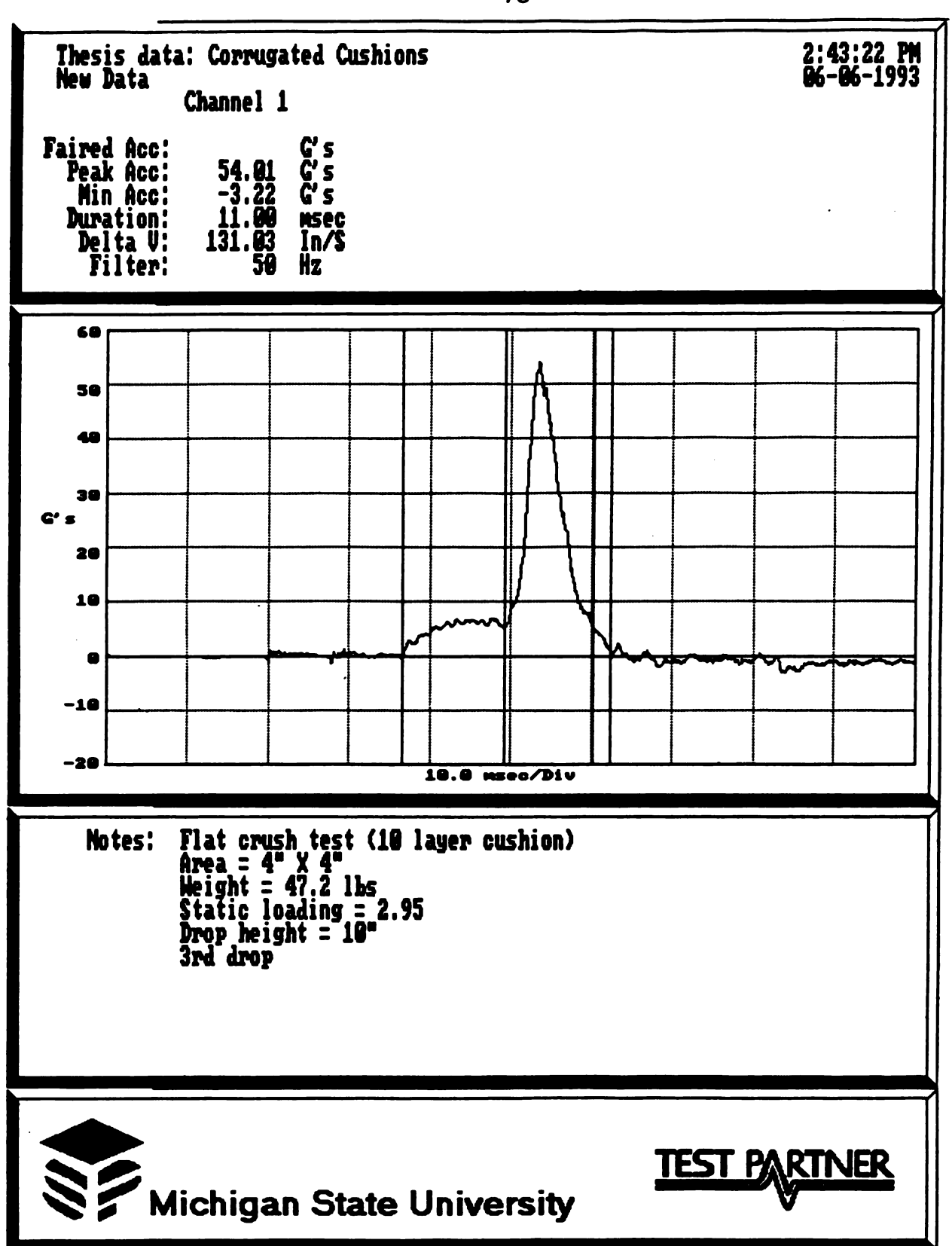
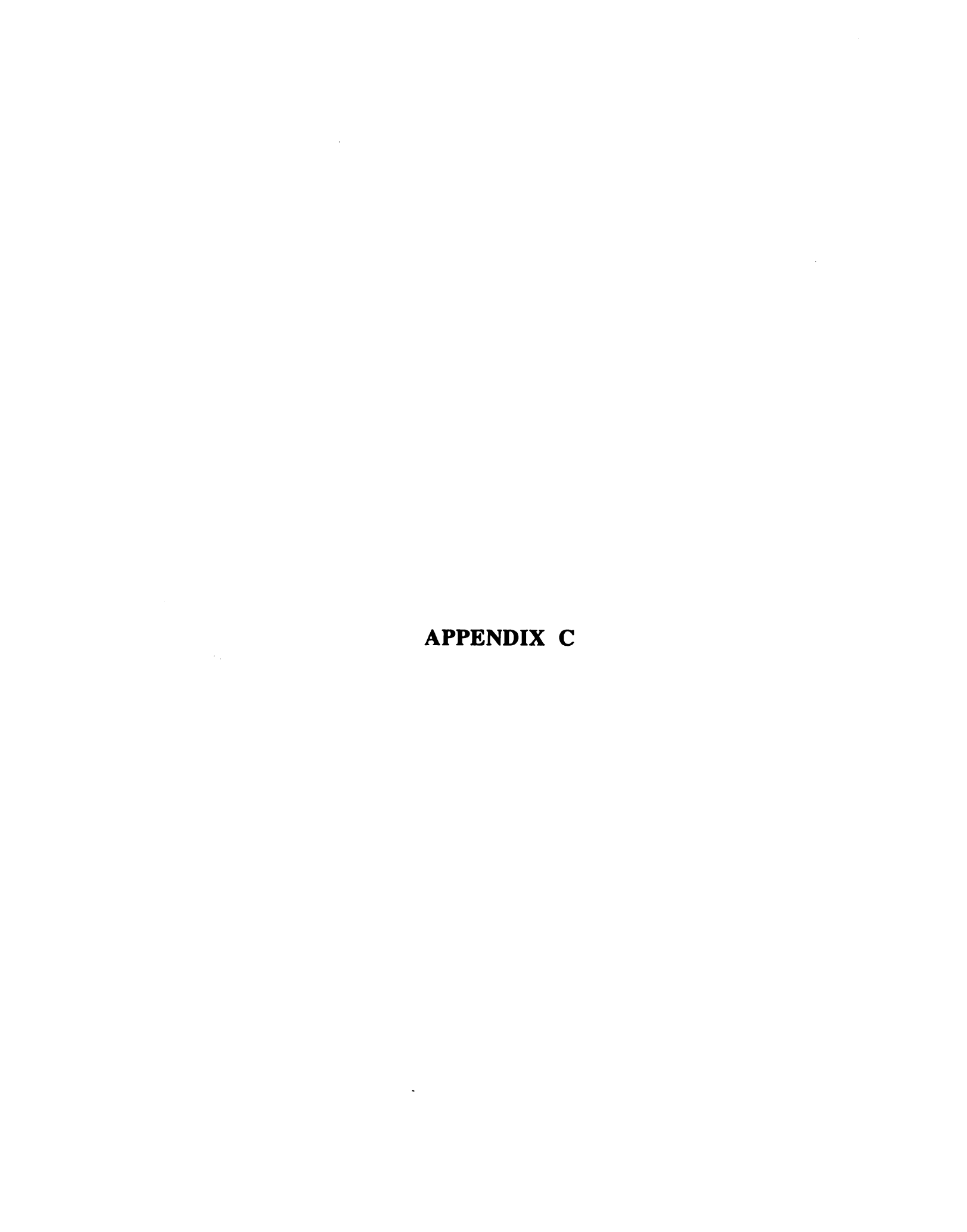


Figure 32: Shock pulse from flat cushion subjected to last drop conditions.



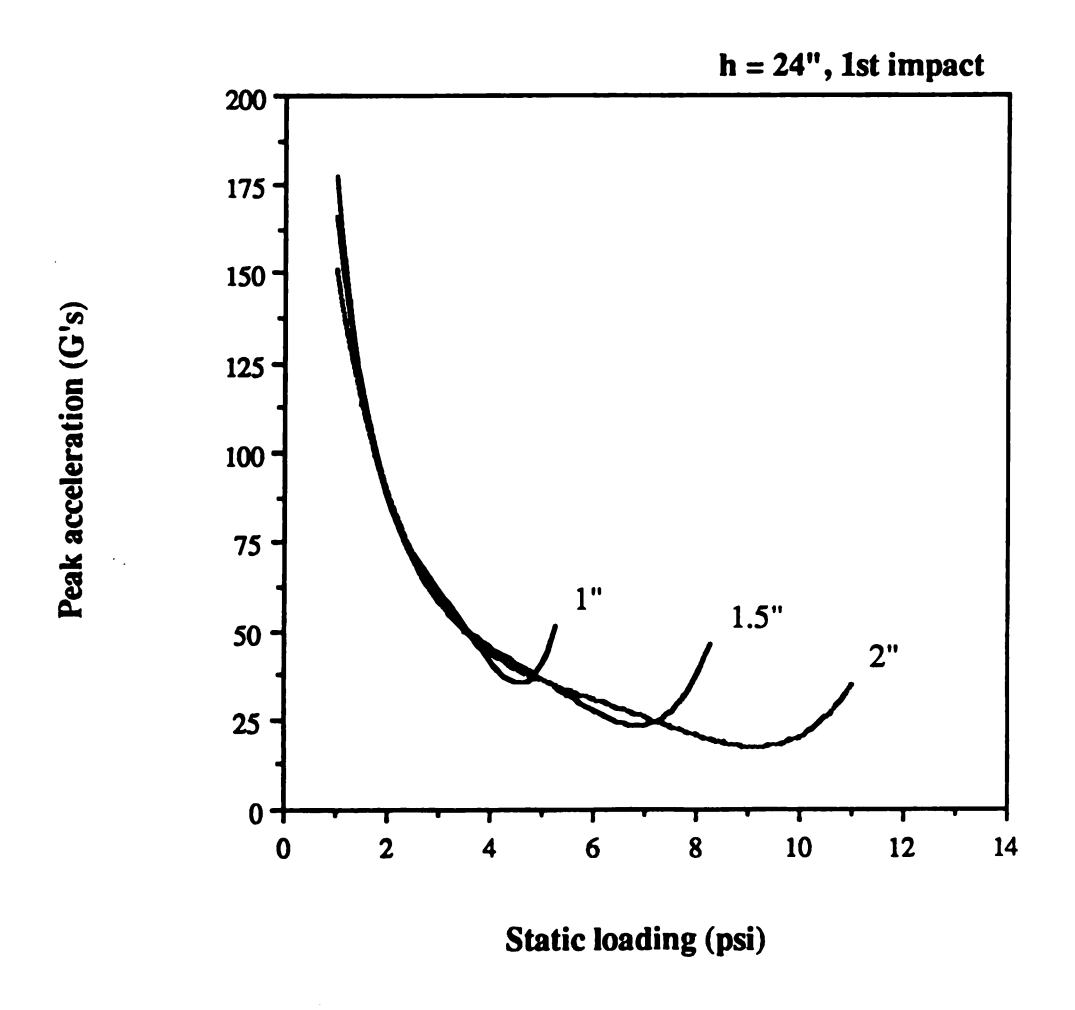


Figure 33: Cushion curve for 24" drop for C-flute board in edge crush mode @ 50% RH.

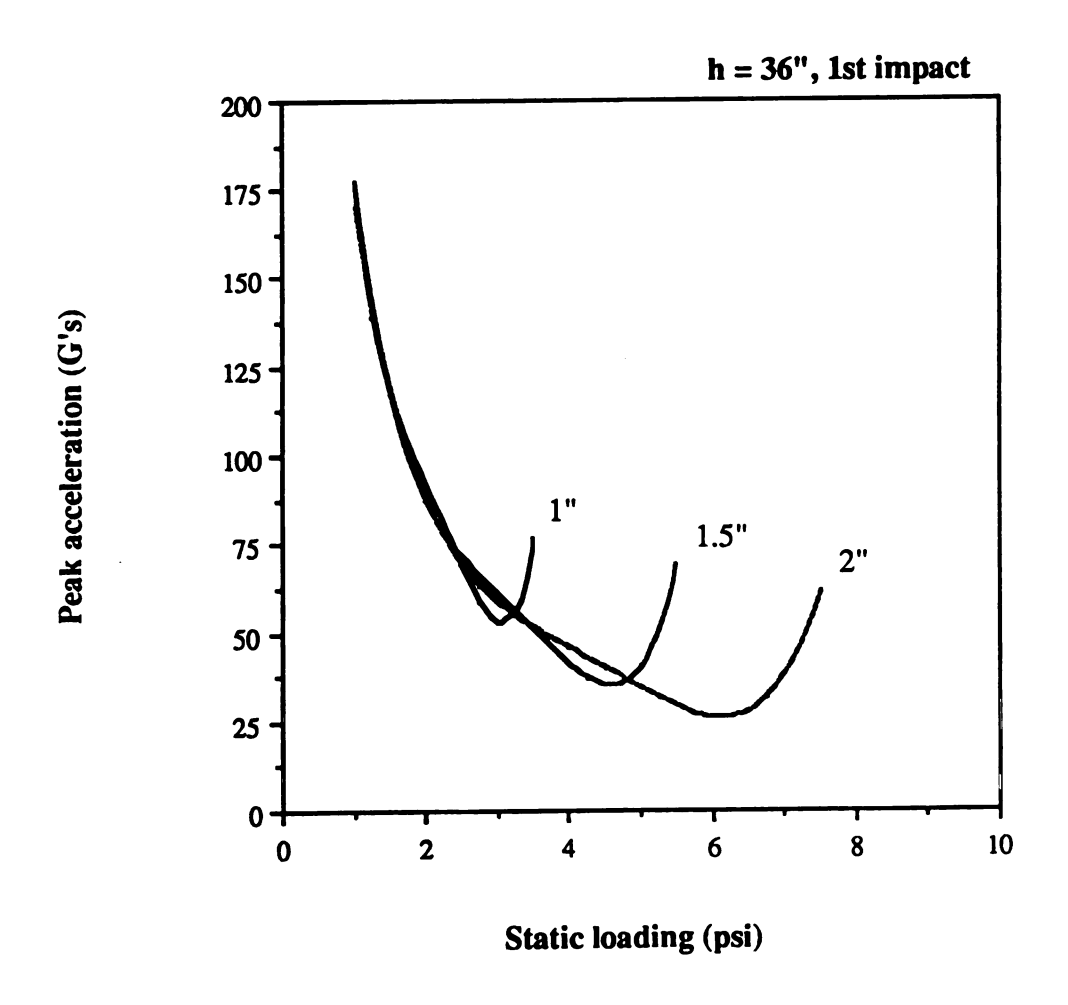
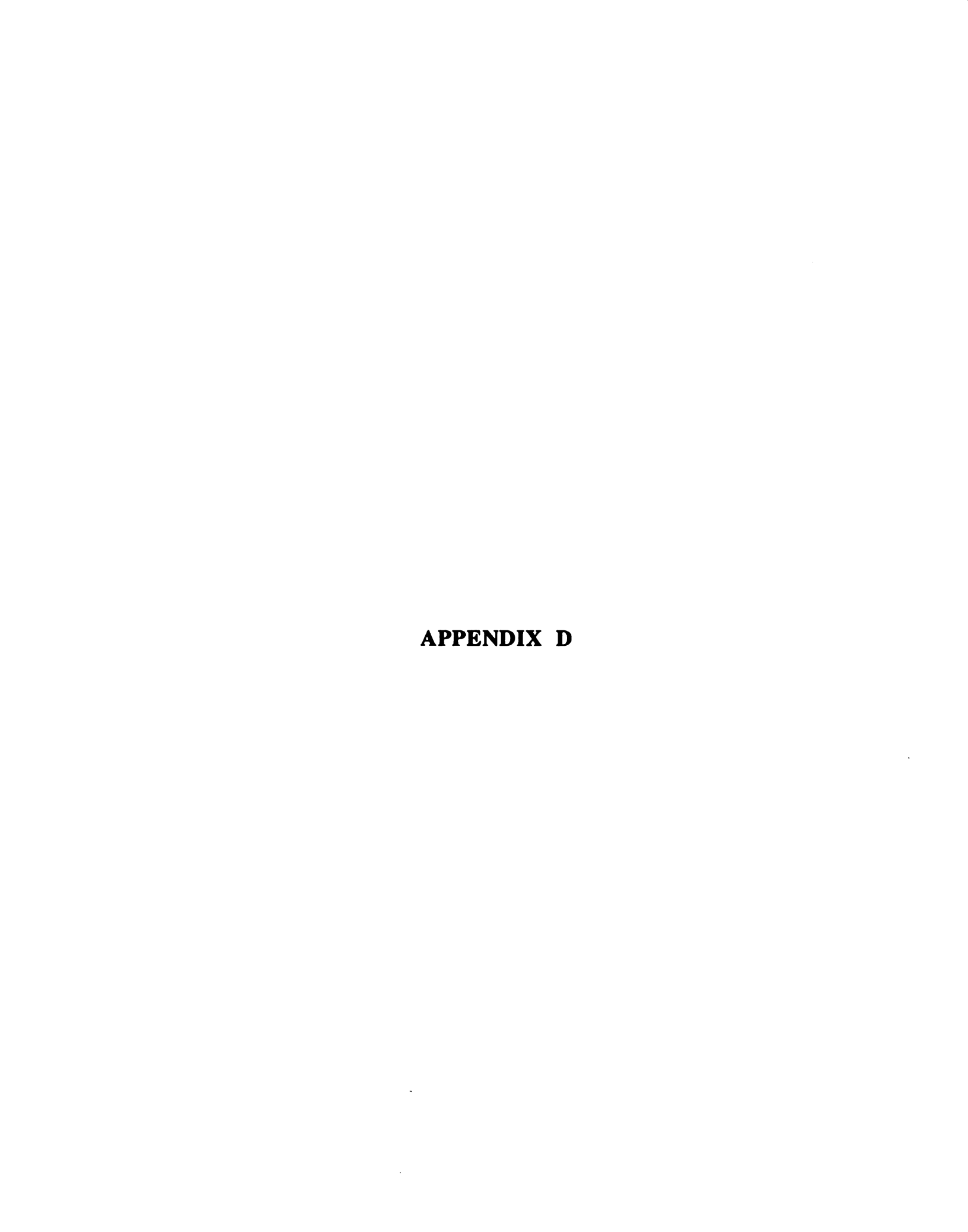


Figure 34: Cushion curve for 36" drop for C-flute board in edge crush mode @ 50% RH.



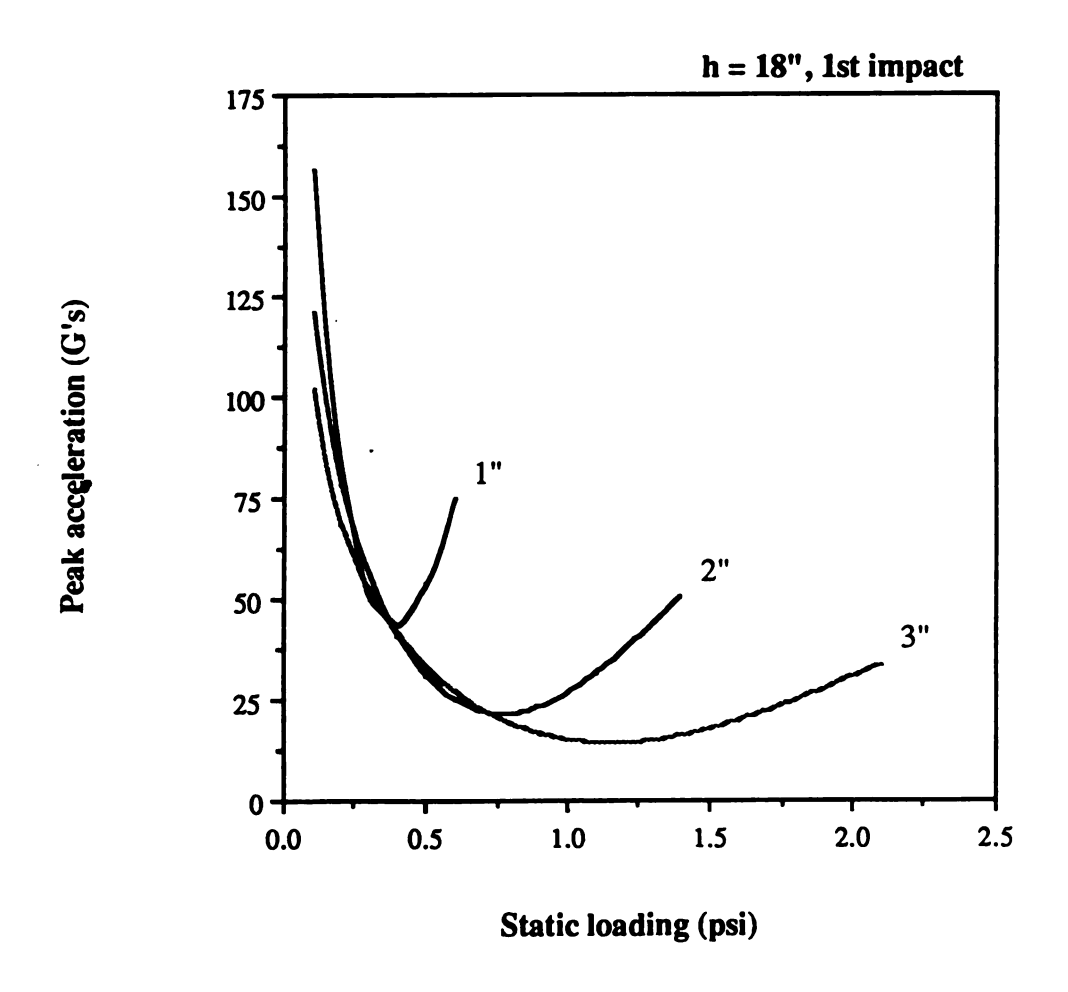


Figure 35: Cushion curve for 18" drop for C-flute board in flat crush mode @ 50% RH.

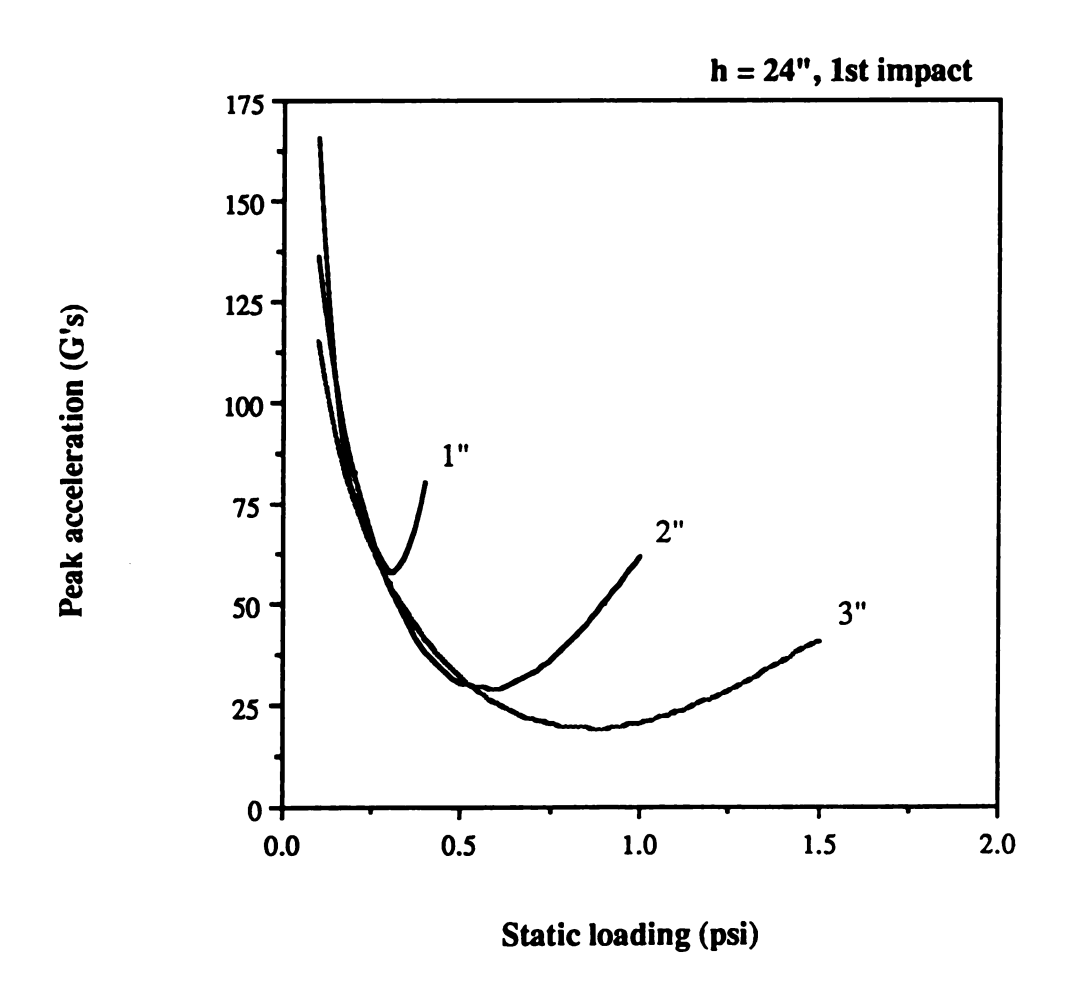
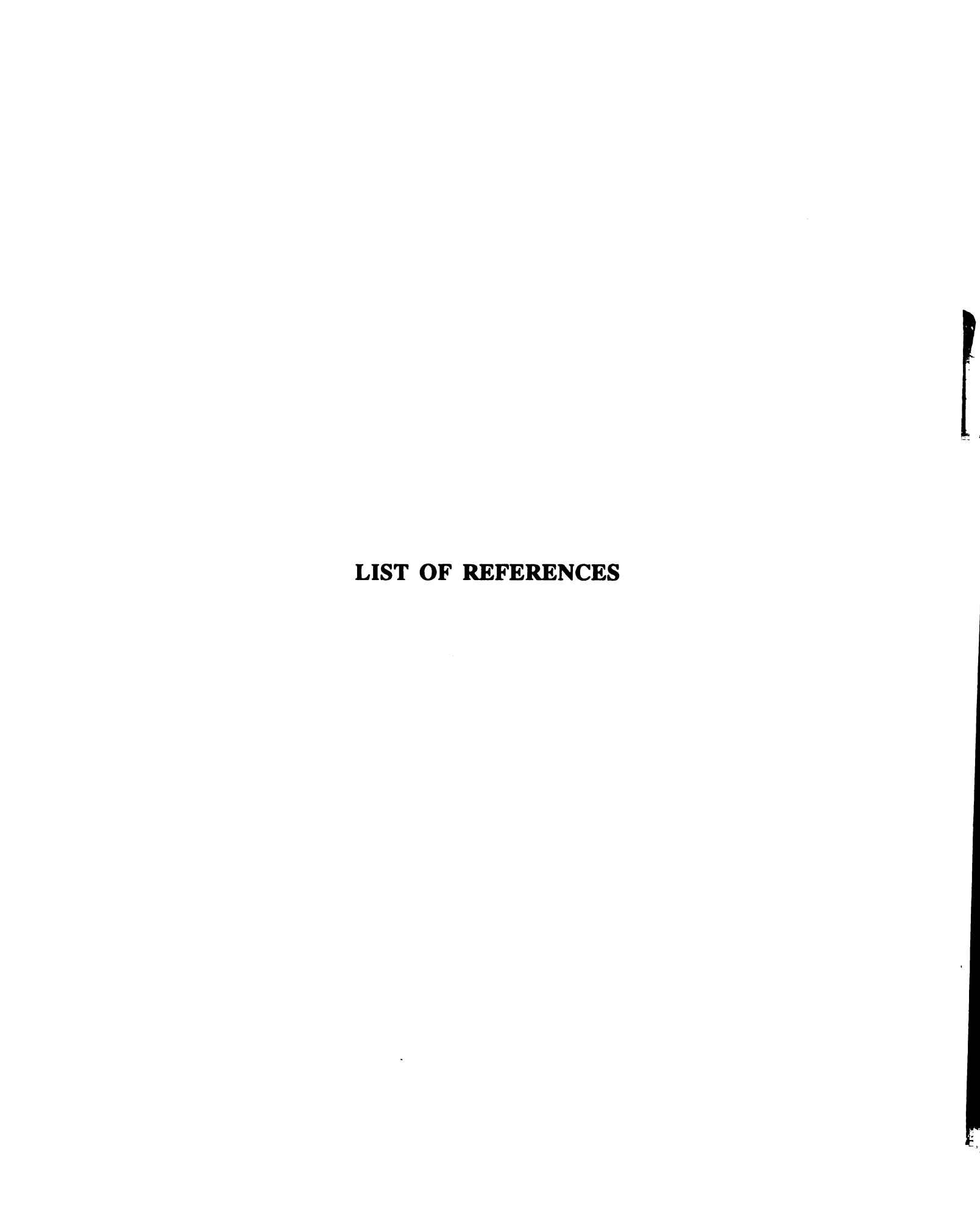


Figure 36: Cushion curve for 24" drop for C-flute board in flat crush mode @ 50% RH.



LIST OF REFERENCES

- 1. Fiber Box Association. Fiber Box Handbook. Rolling Meadows, IL., 1989, p. 2-4.
- 2. Singh, S.P., N. Graham, J. Cornell, "Cushion Testing of Kraft Paper Honeycomb", School of Packaging, Michigan State University, April 1986.
- 3. Asvanit, P., "On the Effect of Moisture Content on the Shock Transmission Properties of Honeycomb Cushioning", Master's Thesis, School of Packaging, Michigan State University, 1988.
- 4. Burgess, G.J., "Thermodynamic Observations on Mechanical Properties of Cushions", Journal of Cellular Plastics (Jan. 1988).
- 5. Throne, J. and R. Progelhof, "Closed-Cell Foam Behavior Under Dynamic Loading-I. Stress-Strain Behavior of Low Density Foams", Journal of Cellular Plastics (Nov./Dec. 1984).
- 6. Ripperger, E.A., "Energy Absorption Characteristics of Paper Honeycomb", Engineering Mechanics Research Laboratory, The University of Texas, Austin, May 18, 1967.
- 7. Witting, R.H., "Investigation of Paperboard Honeycomb Material for Use as Cushioning in Aerial Delivery of Supplies and Equipment", Quartermaster Food and Container Institute for the Armed Forces, Project No. 7-87-03-002, March 9, 1954.
- 8. Karnes, C.H., J.W. Turnbow, E.A. Ripperger, J.N. Thompson, "High Velocity Impact Cushioning, Part V, Energy Absorption Characteristics of Paper Honeycomb", Structural Mechanics Research Laboratory, The University of Texas, Austin, May 1959.

- 9. ASTM D 2808-90, "Compressive Strength of Corrugated Fiberboard", American Society for Testing and Materials, 1991.
- 10. Hanlon, J.F., <u>Handbook of Package Engineering</u>. McGraw-Hill, Inc., 1985, p. 14.2-14.8.
- 11. T 808 om-86, "Flat Crush Test of Corrugated Board", Technical Association of the Pulp and Paper Industry, 1986.
- 12. Burgess, G.J., Advanced Packaging Dynamics-Course Notes, School of Packaging, Michigan State University, 1993.
- 13. Hopf, J.P., "Equilibrium Moisture Content of Paper Honeycomb and Its Effect on Energy Absorption", Forest Products Laboratory, Project No. 7-87-03-004B, Report NO.1, December 1955.
- 14. ASTM D 4332-89, "Conditioning Containers, Packages, or Packaging Components for Testing", American Society for Testing and Materials, 1991.
- 15. ASTM D 1596-91, "Dynamic Shock Cushioning Charactersitics of Packaging Materials", American Society for Testing and Materials, 1991.
- 16. ASTM D 3332-88, "Mechanical-Shock Fragility of Products, Using Shock Machines", American Society for Testing and Materials, 1991.
- 17. Product data: "Dynamic Cushioning Performance", Arpro Moldable Polypropylene, ARCO Chemical CO., Division of Atlantic Richfield CO., Philadelphia, PA 19101.
- 18. Product data: "Dynamic Cushioning Performance", Arcel Moldable Polyethylene Copolymer, ARCO Chemical CO., Division of Atlantic Richfield CO., Philadelphia, PA 19101.